


Research Article

A 25,000 year record of climate and vegetation change from the southwestern Cape coast, South Africa

Lynne J. Quick^{a*} , Brian M. Chase^{b,c}, Andrew S. Carr^d, Manuel Chevalier^e, B. Adriaan Grobler^a and Michael E. Meadows^{c,f,g}

^aAfrican Centre for Coastal Palaeoscience, Nelson Mandela University, Port Elizabeth, Eastern Cape 6031, South Africa; ^bInstitut des Sciences de l'Evolution-Montpellier (ISEM), University of Montpellier, Centre National de la Recherche Scientifique (CNRS), EPHE, IRD, Montpellier, France; ^cDepartment of Environmental and Geographical Science, University of Cape Town, South Lane, Upper Campus, 7701 Rondebosch, South Africa; ^dSchool of Geography, Geology and the Environment, University of Leicester, University Road, Leicester LE1 7RH, UK; ^eInstitut für Geowissenschaften und Meteorologie, Rheinische Friedrich-Wilhelms-Universität Bonn, Auf dem Hügel 20, 53121 Bonn, Germany; ^fSchool of Geographic Sciences, East China Normal University, 500 Dongchuan Road, Shanghai 200241, PR China and ^gCollege of Geography and Environmental Sciences, Zhejiang Normal University, Jinhua 321004, PR China

Abstract

The southwestern Cape of South Africa is a particularly dynamic region in terms of long-term climate change. We analysed fossil pollen from a 25,000 year sediment core taken from a near-coastal wetland at Pearly Beach that revealed that distinct changes in vegetation composition occurred along the southwestern Cape coast. From these changes, considerable variability in temperature and moisture availability are inferred. Consistent with indications from elsewhere in southwestern Africa, variability in Atlantic Meridional Overturning Circulation (AMOC) was identified as a strong determinant of regional climate change. At Pearly Beach, this resulted in phases of relatively drier conditions (~24–22.5 cal ka BP and ~22–18 cal ka BP) demarcated by brief phases of increased humidity from ~24.5–24 cal ka BP and 22.5–22 cal ka BP. During glacial Termination I (~19–11.7 ka), a marked increase in coastal thicket pollen from ~18.5 to 15.0 cal ka BP indicates a substantial increase in moisture availability, coincident, and likely associated with, a slowing AMOC and a buildup of heat in the southern Atlantic. With clear links to glacial and deglacial Earth system dynamics and perturbations, the Pearly Beach record represents an important new contribution to a growing body of data, providing insights into the patterns and mechanisms of southwestern African climate change.

Keywords: Last glacial maximum, Heinrich stadial 1, Atlantic meridional overturning circulation, Climate change, Vegetation dynamics, South Africa

(Received 20 November 2020; accepted 20 April 2021)

INTRODUCTION

The southwestern Cape of South Africa is a particularly dynamic region in terms of long-term climate change, as it is situated at the nexus of the three dominant climate systems in southern Africa: the South Atlantic anticyclone, the temperate westerlies, and the tropical easterlies (Tyson, 1986; Taljaard, 1996; Tyson and Preston-Whyte, 2000; Chase and Meadows, 2007). While most of the subcontinent experiences summer rainfall as a result of perturbations in the tropical easterlies, the southwestern Cape presently receives the majority of its rainfall during the austral winter, when the southern westerly storm track migrates northward (Tyson, 1986; Taljaard, 1996; Tyson and Preston-Whyte, 2000). In contrast, during the austral summer, the westerlies and the South Atlantic Anticyclone shift southward limiting the influence of both frontal systems and tropical moisture sources (Tyson and

Preston-Whyte, 2000; Reason et al., 2006). These spatially distinct precipitation patterns led to the classification of the winter rainfall zone (WRZ) (*sensu* Chase and Meadows, 2007; >66% of annual precipitation in winter), the summer rainfall zone (SRZ; >66% of annual precipitation in summer), and a transitional zone of limited seasonality between the WRZ and SRZ, the aseasonal or year-round rainfall zone (ARZ) (Fig. 1).

The southwestern Cape is also where the warm Agulhas Current and the cold Benguela Current meet and, the region is thus also particularly dynamic from an oceanographic perspective. Both currents are key components of the global ocean “conveyor belt” (thermohaline circulation) (Lutjeharms, 1996; Rahmstorf, 2006) and therefore contribute not only to climatic variability within the southwestern Cape but also play a role in global climate dynamics (Walker, 1990; Walker and Shillington, 1990; Cohen and Tyson, 1995; Reason, 2001; Biastoch et al., 2009; Beal et al., 2011).

The climatic setting of the southwestern Cape has played an important part in the development of the vegetation of the Cape Floristic Region (CFR) and is thought to have fostered the region's extraordinary botanical diversity (Goldblatt, 1978; Linder et al., 1992; Cowling and Lombard, 2002; Linder, 2005; Bradshaw and Cowling, 2014; Cowling et al., 2015). While long-term climatic

*Corresponding author: African Centre for Coastal Palaeoscience, Nelson Mandela University, Port Elizabeth, Eastern Cape 6031, South Africa. E-mail address: lynne.quick@gmail.com (L.J. Quick).

Cite this article: Quick LJ, Chase BM, Carr AS, Chevalier M, Grobler BA, Meadows ME (2022). A 25,000 year record of climate and vegetation change from the southwestern Cape coast, South Africa. *Quaternary Research* 105, 82–99. <https://doi.org/10.1017/qua.2021.31>

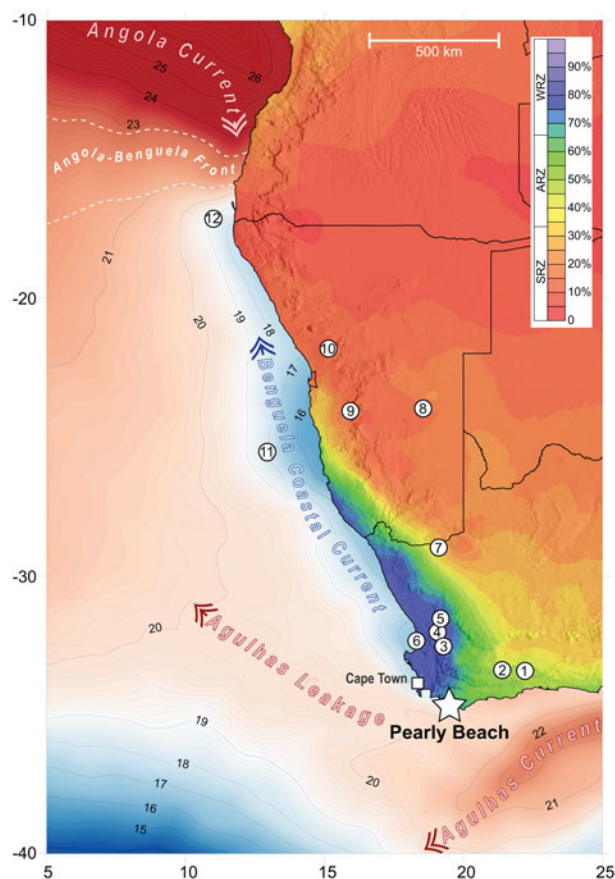


Figure 1. Map of the southwestern margin of Africa showing seasonality of rainfall and sharp climatic gradients dictated by the zones of summer/tropical (red) and winter/temperate (blue) rainfall dominance. The major oceanic circulation systems (the cold Benguela Current and the warm Agulhas and Angola Currents; temperatures shown in °C; Reynolds et al., 2007) are indicated, as well as the position of Pearly Beach (star) in relation to key palaeoclimatic records. 1, Cango Caves (Talma and Vogel, 1992); 2, Seweweekspoort (Chase et al., 2013, 2017); 3, Katbakkies Pass (Meadows et al., 2010; Chase et al., 2015b); 4, De Rif (Chase et al., 2011, 2015a; Quick et al., 2011; Valsecchi et al., 2013); 5, Pakhuis Pass (Scott and Woodborne, 2007a, 2007b; Chase et al., 2019a); 6, Elands Bay Cave (Cowling et al., 1999; Parkington et al., 2000); 7, Pella (Lim et al., 2016; Chase et al., 2019b); 8, Stampriet Aquifer (Stute and Talma, 1998); 9, Zizou (Chase et al., 2019b); 10, Spitzkoppe (Chase et al., 2009, 2019b); 11, ODP 1084B (Farmer et al., 2005); 12, GeoB 1023-5 (Kim et al., 2003).

stability during the Pliocene and Pleistocene is hypothesised to be one of the key factors for the diversification of the Cape flora (Cowling et al., 1997, 2015; Cowling and Lombard, 2002; Linder, 2005; Bergh and Cowling, 2014), little direct evidence is available. Furthermore, species diversity within the CFR is not homogeneous, and at finer spatial and temporal scales, the concept of climatic stability driving diversity and species richness becomes more complex (Cowling, 1992; Cowling et al., 1997; Cowling and Lombard, 2002). Palaeoclimatic records from the western montane region of the CFR provide evidence for steep palaeoenvironmental gradients and highlight the need for more research to be conducted to assess the role of palaeoclimatic change in biodiversity patterns (Chase et al., 2019a).

Despite the challenges of conducting Quaternary palaeoenvironmental studies in arid–semi-arid areas (see Chase and Meadows, 2007), considerable progress has been made over the last decade in terms of the generation of high-resolution

palaeoclimatic records for the southwestern and southern Cape regions (e.g., Neumann et al., 2011; Stager et al., 2012; Chase et al., 2013, 2015a, 2019a, 2020; Valsecchi et al., 2013; Quick et al., 2018; Wündsche et al., 2018; Kirsten et al., 2020). This emerging regional data set is enabling a more refined understanding of the spatial and temporal complexity of climate and vegetation responses to a range of forcing mechanisms and suggests that substantial variability in inferred climatic trends/trajectories occurs across relatively short distances (e.g., Chase et al., 2015a, 2017, 2020; Chase and Quick, 2018). Even though more—and indeed more detailed—records are now available, most of these records only cover the Holocene (11.7–0 cal ka BP) or portions thereof. In particular, greater spatial and temporal coverage is still needed to fully document the last glacial maximum (LGM; 26.5–19 ka; Clark et al., 2009) and last glacial termination (Termination I; the period from the end of the LGM to the early Holocene, ~19–11.7 ka).

During Termination I, one of the primary internal drivers of global change was variability in Atlantic Meridional Overturning Circulation (AMOC), a key component of the thermohaline circulation (Mix et al., 1986; Crowley, 1992; Broecker, 1998; Stocker, 1998; Stocker and Johnsen, 2003). The AMOC transports heat from the Southern Hemisphere to the North Atlantic basin. Perturbations in the strength of the AMOC thus impact climate in both hemispheres, with a stronger AMOC resulting in net cooling (warming) in the Southern (Northern) Hemisphere, and a weaker AMOC resulting in a buildup of heat in the Southern Hemisphere while the Northern Hemisphere cools, a dynamic referred to as the “bipolar seesaw” (Broecker, 1998; Stocker and Johnsen, 2003). Massive ice and freshwater discharges in the North Atlantic, known as Heinrich events, exerted a significant influence on the AMOC, resulting, for example, in its near shutdown during Heinrich stadial 1 (HS1; ~18–14.6 ka) (Broecker, 1998; McManus et al., 2004; Ritz et al., 2013; Ng et al., 2018; Bendle et al., 2019).

In the southwest African sector, the influence of a weaker AMOC is manifested in a general warming of southeast Atlantic sea-surface temperatures (SSTs) (Kim and Schneider, 2003; Farmer et al., 2005), a poleward shift of the Subtropical Front (Barker et al., 2009), and thus likely an increase in Agulhas leakage (Gordon, 1986; Peeters et al., 2004; Caley et al., 2012; Rühls et al., 2019). As an example, the abrupt slowdown in the AMOC during HS1 is consistent as the underlying driver for the distinct humid phase registered at sites along the western continental margin in the Namib Desert (Lim et al., 2016; Chase et al., 2019b) and the Cederberg Mountains in the southwestern Cape (Chase et al., 2015a), as well as further afield in the continental interior (Chase et al., 2017; Chevalier and Chase, 2015). It remains to be determined, however, how these changes in the AMOC affected Africa’s southern/southwestern Cape coast, particularly in the context of the emerging evidence for spatial complexity in the regional climatic response (Chase and Quick, 2018; Chase et al., 2019a, 2020). This brings into question the utility of the simple widely used binary models that indicate or infer a coeval inverse relationship between the WRZ and SRZ (van Zinderen Bakker, 1976; Cockcroft et al., 1987) and thus how climate changes related to the AMOC may have manifested in the region.

To investigate the potential influence of AMOC variability at the interface of the Agulhas and Benguela Currents and at the margin of the WRZ, we present here a new record of fossil pollen, charcoal, and sediment grain size from a 25,000 year sediment core taken from Pearly Beach 1, a near-coastal wetland site

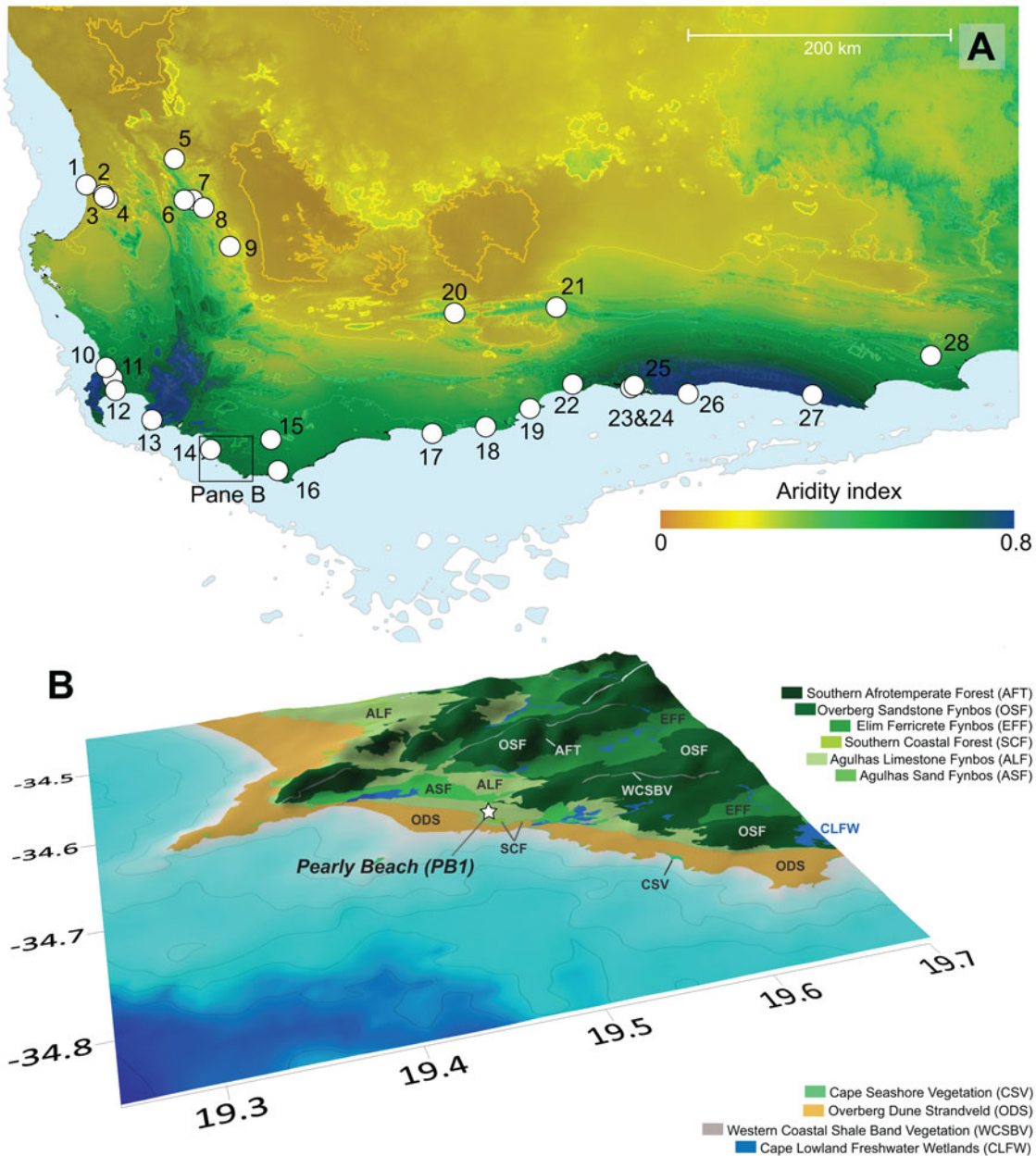


Figure 2. (A) Aridity index map of the southwestern Cape (data: Zomer *et al.*, 2008), with lower values indicating drier conditions. Peripheral blue shading indicates position of shoreline at last glacial maximum (LGM) low stand (−130 m). The locations of published palaeoenvironmental and archaeological records from the region are shown: 1, Elands Bay Cave (Parkington *et al.*, 1988, 2000; Cowling *et al.*, 1999); 2, Grootdrift (Meadows *et al.*, 1996); 3, Verlorenvlei (Kirsten *et al.*, 2020; Stager *et al.*, 2012; Carr *et al.*, 2015); 4, Klaarfontein Springs (Meadows and Baxter, 2001); 5, Pakhuis Pass (Scott and Woodborne, 2007a, 2007b); 6, Sneeuwberg Vlei and Driehoek Vlei (Meadows and Sugden, 1991); 7, De Rif (Chase *et al.*, 2011, 2015a; Quick *et al.*, 2011; Valsecchi *et al.*, 2013); 8, Truitjes Kraal (Meadows *et al.*, 2010); 9, Katbakkies (Meadows *et al.*, 2010; Chase *et al.*, 2015b); 10, Rietvlei (Schalke, 1973); 11, Cape Flats (Schalke, 1973); 12, Princess Vlei (Neumann *et al.*, 2011; Kirsten and Meadows, 2016; Cordova *et al.*, 2019); 13, Cape Hangklip (Schalke, 1973); 14, Die Kelders (Klein and Cruz-Uribe, 2000); 15, Bynekranskop (Schweitzer and Wilson, 1982; Faith *et al.*, 2018); 16, Agulhas Plain vleis and lunettes (Soetendalsvlei, Voëlvlei, Renosterkop, and Soutpan) (Carr *et al.*, 2006a, 2006b); 17, Blombos Cave (Henshilwood *et al.*, 2001); 18, Rietvlei-Still Bay (Quick *et al.*, 2015); 19, Pinnacle Point (Marean, 2010; Rector and Reed, 2010); 20, Seweweekspoort (Chase *et al.*, 2013, 2017); 21, Cango Cave (Talma and Vogel, 1992) and Boomplaas Cave (Deacon *et al.*, 1984); 22, Norga peats (Scholtz, 1986); 23, Eilandvlei (Kirsten *et al.*, 2018; Quick *et al.*, 2018; Wündsche *et al.*, 2018) and Bo Langvlei (du Plessis *et al.*, 2020); 24, Groenvlei (Martin, 1968; Wündsche *et al.*, 2016); 25, Vankervelsvlei (Irving and Meadows, 1997; Quick *et al.*, 2016); 26, Nelson Bay Cave (Cohen and Tyson, 1995); 27, Klasies River Mouth (Deacon *et al.*, 1986) and 28 Uitenhage Aquifer (Heaton *et al.*, 1986; Stute and Talma, 1998). (B) Location of Pearly Beach 1 sediment coring site in relation to the current distribution of dominant vegetation types (South African National Biodiversity Institute, 2018). Bathymetry contours are at 20 m intervals (GEBCO Bathymetric Compilation Group, 2020) and 0.1° grid intervals equate to ~9.2 km at this latitude.

situated on the eastern coastal boundary of the present-day WRZ (Figs. 1 and 2). Data from the core present a rare opportunity to consider vegetation/climate responses through this major global climate transition. The record reveals that distinct changes in

vegetation composition occurred along the southwestern Cape coast during the LGM, Termination I, and the Holocene. From these data, we infer considerable variability in temperature and moisture availability over the last 25,000 years and link these

changes to glacial and interglacial boundary conditions, and particularly to the perturbations and dynamics in the Earth system that characterised the process of deglaciation.

REGIONAL SETTING

In 2007, a sediment core (Pearly Beach 1, referred to hereafter as PB1; 34°38.880'S; 19°30.300'E, 5 m above sea level [m asl], 2.5 km from the current coastline; Fig. 2) was extracted from wetlands 2 km north of the coastal town of Pearly Beach, ~200 km southeast of Cape Town. The site is situated on the boundary of the modern WRZ (*sensu* Chase and Meadows, 2007; >66% of annual precipitation falling in MJJAS), receiving 68% of its mean annual average of ~450 mm of rainfall during the winter (Climate System Analysis Group, 2021). Temperatures are moderate (monthly averaged daily mean of 17°C), snow has not been recorded, and frost appears to be absent from the area as well.

The Pearly Beach wetland complex is situated on a low-lying undulating coastal plain that is bounded to the north by Bredasdorp Group limestone (calcareous) ridges and Table Mountain Group sandstone outcrops of the Peninsula Formation (Malan, 1990). The wetlands derive their waters from the limestone uplands to the northeast of the site via both runoff and throughflow from spring seeps. Transverse coastal dunes, currently invaded by extensive alien vegetation, stretch along the southern and western boundaries of the wetland adjacent to the ocean. Relict deflated parabolic dunes can be identified within the landscape towards the northwest and southeast of the site. The coastal platform is underlain by unconsolidated aeolian calcareous Quaternary sediments of the Strandveld Formation with partially consolidated calcrete lenses found in some patches along the coast and further inland (Gresse and Theron, 1992). Alluvial deposits characterise the wetlands of the area. On the limestone ridges, soils are shallow, alkaline, and calcareous, whereas the lower slopes are characterised by more acidic, colluvial soils with evidence of early stages of podsolisation (Rebelo et al., 1991). The young coastal dune sands are associated with deeper calcareous, alkaline soils in comparison to the soils found on the slopes.

Contemporary vegetation

The study area (Fig. 2) is home to the Groot Hagelkraal farm—a registered private nature reserve and a South African Nature Foundation Natural Heritage Site. The Groot Hagelkraal area harbours six local-endemic and 21 regional-endemic plant species and has been lauded as the world's "hottest" biodiversity hotspot and foremost conservation priority in the CFR (Cowling, 1996; Willis et al., 1996; Jones et al., 2002). The surrounding landscape is dominated by (1) sclerophyllous, Mediterranean-type shrublands of the fynbos biome, found on both the lowlands and uplands; (2) subtropical thickets that occupy parts of the near-coastal dune fields adjacent to the site; and (3) pockets of forest vegetation in more sheltered sites (Cowling et al., 1988; Mucina and Rutherford, 2006). Where surface water is perennially or seasonally available, lowland areas also support riparian and wetland habitats (Mustart et al., 2003).

The azonal vegetation associated with the wetland systems around Pearly Beach and the upper reaches of the Groot Hagelkraal River is broadly classified as Cape Lowland Freshwater Wetlands (Mucina et al., 2006b). These systems are dominated by the reed *Phragmites australis* (Poaceae) and the rushes *Juncus kraussii* and *Juncus capensis* (Juncaceae). Sedges, especially *Ficinia nodosa* (Cyperaceae), form dense stands along

the margins of the vlei, while *Typha capensis* and *Isolepis prolifera* (Cyperaceae) inhabit the open water and shallower margins, together with obligate aquatics like *Aponogeton distachyos* and *Nymphaea nouchali*.

Three broad types of fynbos vegetation occur in the study area, each associated with a specific edaphic substrate (Thwaites and Cowling, 1988). Agulhas Limestone Fynbos occurs in fragmented patches inland of the Pearly Beach site on shallow, alkaline sands that accumulate in depressions over Bredasdorp Group limestone pavements (Cowling et al., 1988; Mustart et al., 2003; Rebelo et al., 2006). This mid-high, moderately dense shrubland contains tall, emergent proteoids and is characterised by the presence of *Protea obtusifolia* and *Leucadendron meridianum*. The restioid component is poorly developed, but the widespread species *Elegia microcarpa* and *Restio leptoclados* and the more restricted *Thamnochortus fraternus* are typical of this fynbos type. Typical ericoid shrubs include *Aspalathus calcarea* (Fabaceae), *Metalasia calcicola* (Asteraceae), *Phyllica selaginoides*, and *Passerina paleacea*, as well as several local- and regional-endemic species of the Ericaceae (e.g., *Erica calciphila*) and Rutaceae (e.g., *Diosma haelkraalensis*) (Mustart et al., 2003; Rebelo et al., 2006).

Like Agulhas Limestone Fynbos, Agulhas Sand Fynbos is associated with Bredasdorp Group limestones, but this vegetation type occurs on deep colluvial, neutral sands that fringe the base of limestone outcrops (Cowling et al., 1988; Mustart et al., 2003; Rebelo et al., 2006). Overstorey proteoids that characterise this vegetation type are *Protea susannae* and *Leucadendron coniferum*. Typical ericoid shrubs include *Erica discolor*, *Erica plukenetii* subsp. *lineata*, *Metalasia densa*, and *Passerina corymbosa*, as well as the Hagelkraal-endemic *Spatalla ericoides* (Mustart et al., 2003; Rebelo et al., 2006). Commonly occurring restioids are *Elegia filacea*, *Elegia tectorum*, *Restio triticeus*, *Thamnochortus erectus*, and *Thamnochortus insignis*.

Overberg Sandstone Fynbos occurs on the rolling uplands, where it is associated with deep colluvial, infertile acid sands derived from Table Mountain Group sandstones (Thwaites and Cowling, 1988; Cowling et al., 1988; Rebelo et al., 2006; Fig. 2). *Protea compacta* is the dominant and characteristic overstorey proteoid, while *Leucadendron xanthoconus* is also common. Restioids can be locally abundant, with *Ceratocaryum argenteum*, *Hypodiscus argenteus*, *Mastersiella digitata*, and *Staberoha multispicula* being typical species.

The deep, well-drained alkaline sands of coastal dunes in the study area support Overberg Dune Strandveld, a mosaic-type vegetation comprising small clumps of subtropical thicket in a matrix of asteraceous fynbos (Cowling et al., 1988; Rebelo et al., 2006). The dune-fynbos component is dominated by non-ericaceous ericoid shrubs, especially *Acmadenia obtusata* (Rutaceae), *Agathosma collina* (Rutaceae), *Metalasia muricata* (Asteraceae), *Muraltia satureioides* (Polygalaceae), *P. paleacea*, and *Phyllica ericoides* (Mustart et al., 2003). Restioids are not abundant in the dune fynbos; this group is typically represented by only two species, *E. microcarpa* and *Restio eleocharis*. A conspicuous difference between the fynbos component of Overberg Dune Strandveld and the other fynbos vegetation types occurring in the study area is the absence of proteoids in the former (Cowling et al., 1988). While subtropical thicket shrubs occur throughout Overberg Dune Strandveld, dune thicket clumps are best developed in moist, wind- and fire-protected dune slacks, where their structure and composition approach that of coastal forests (see below). Characteristic dune thicket shrubs include *Carissa bispinosa* (Apocynaceae), *Euclea racemosa*, *Morella*

Table 1. Accelerator mass spectrometry (AMS) radiocarbon ages for Pearly Beach 1.^a

Lab code	Average depth (cm)	¹⁴ C age BP	1σ error	95.4% (2σ) cal age range	Median probability (cal BP)
Beta-298974	23.0	540	30	548–502	525
Beta-305128	72.5	7410	40	83195–8045	8188
Beta-311274	100.5	11,080	50	13,044–12,752	12,901
Beta-298973	121.5	12,046	50	14,027–13,735	13,859
Beta-298972	167.5	17,800	80	21,801–21,206	21,505
Beta-305127	207.0	19,420	90	24,498–23,986	23,330
Beta-298971	227.3	20,220	90	23,613–23,023	24,244
Beta-308917	229.8	20,160	80	24,424–23,938	24,183

^aThe SHCal13 dataset (Hogg et al., 2013) was used to calibrate the ages.

cordifolia, *Myrsine africana*, *Lauridia tetragona* (Celastraceae), *Olea exasperata*, *Robsonodendron maritimum* (Celastraceae), *Pterocelastrus tricuspidatus* (Celastraceae), and *Searsia glauca* (Cowling et al., 1988; Mustart et al., 2003; Rebelo et al., 2006).

The azonal vegetation associated with coastal strands, rocky shorelines, and mobile dune cordons in the study area is classified as Cape Seashore Vegetation (Mucina et al., 2006a). Sandy areas typically host the grasses *Ehrharta villosa* and *Thinopyrum distichum* (both Poaceae); the succulent shrubs *Tetragonia decumbens* and *Carpobrotus acinaciformis* (both Aizoaceae); several herbaceous species like *Arctotheca populifolia* (Asteraceae), *Dasispermum suffriticosum* (Apiaceae), *Senecio elegans* (Asteraceae), and *Silene crassifolia* (Caryophyllaceae); and the shrubs *Hebenstreitia cordata* (Scrophulariaceae), *M. cordifolia*, and *Passerina rigida* (Mustart et al., 2003; Mucina et al., 2006a). The more stabilised dunes half a kilometre inland of the littoral zone are predominantly vegetated by *Osteospermum moniliferum* (Asteraceae), which, together with other woody species like *Searsia crenata*, form small pockets of wind-pruned thicket. Along rocky shores, the vegetation comprises low grasslands of salt-tolerant species like *Sporobolus virginicus* and *Stenotaphrum secundatum* or succulent herblands where *Dimorphotheca fruticosa* (Asteraceae), *Drosanthemum intermedium* (Aizoaceae), *Mesembryanthemum vanrensburgii* (Aizoaceae), and *Plantago crassifolia* are typical.

There are small, isolated patches of Southern Coastal Forest to the west of the site that are dominated by *Sideroxylon inerme*. Other trees and shrubs present in these patches include *Cassine peragua* (Celastraceae), *Chionanthus foveolatus* (Oleaceae), *R. maritimum* (Celastraceae), *Maytenus procumbens* (Celastraceae), *Olea capensis*, *Polygala myrtifolia*, *P. tricuspidatus* (Celastraceae), and *Tarchonanthus littoralis* (Asteraceae) (Mustart et al., 2003; Mucina and Geldenhuys, 2006).

MATERIALS AND METHODS

Chronology

The age–depth model for the PB1 core was constructed from eight radiocarbon ages (Table 1). Subsamples of approximately 1 g were taken from various positions along the PB1 core and sent to Beta Analytic Inc. for accelerator mass spectrometry (AMS) radiocarbon dating. These ages were calculated using the Libby half-life of 5568 years following Stuiver and Polach (1977). The ages were corrected for isotope fractionation using the AMS-measured $\delta^{13}\text{C}$, which accounts for both natural and machine fractionation.

The age–depth model was developed in the software package rbacon (v. 2.3.6; Blaauw and Christen, 2011). Using a Bayesian framework, rbacon divides the core into sections and models the accumulation rate for each section through multiple Markov chain Monte Carlo iterations. The ages were calibrated with the SHCal13 data (Hogg et al., 2013).

Particle size analysis

Particle size analysis was conducted at the Department of Geography, Friedrich-Schiller-University, Jena, Germany. Subsamples of ~5 g were pretreated with hydrogen peroxide (H₂O₂) to remove organic material, while carbonates were removed with hydrochloric acid (HCl). Sodium pyrophosphate (Na₄P₂O₇) was added as a deflocculant. The particle size distributions were detected using a Beckman Coulter LS 13 320 Laser Diffraction Particle Size Analyzer, the single-wavelength Aqueous Liquid Module. Measurements were carried out in several runs until a reproducible signal was obtained.

Pollen and microcharcoal analyses

Pollen and microcharcoal subsamples (1 cm thick) were initially taken at 5 cm intervals. This was followed by finer-resolution subsampling at targeted locations along the core that were identified by the initial pollen results as representing periods of significant vegetation change.

Palynomorphs were concentrated and extracted following Moore et al. (1991) with specific adaptations for dense media separation from Nakagawa et al. (1998). This involved 30% HCl treatment to remove carbonates, 10% KOH digestion to disaggregate the samples and remove humic acids, and heavy liquid mineral separation using ZnCl₂ to separate the pollen grains from the non-pollen matrix (Faegri and Iversen, 1989; Moore et al., 1991; Nakagawa et al., 1998). Samples were acetolysed and mounted in Aquatex, an aqueous mounting agent. Three slides were produced per sample, and absolute pollen concentrations were calculated via the addition of *Lycopodium* spores as per Stockmarr (1971). Pollen counts of 500 grains per sample were carried out at 400× magnification for routine identification and 1000× for specific identification. Non-pollen palynomorphs were counted but not included in the total pollen sum. The University of Cape Town pollen reference collection and published resources (van Zinderen Bakker, 1953, 1956; van Zinderen Bakker and Coetzee, 1959; Scott, 1982) were used for the identification of pollen taxa. The pollen and microcharcoal diagram was constructed

in Tilia (v. 2.1.1) (Grimm, 1991) and was divided into statistically significant pollen assemblage zones based on a constrained incremental sum of squares (CONISS; with square-root transformation) analysis (Grimm, 1987).

Charcoal particles were identified and counted on the same microscope slides produced for the pollen analysis. Only particles that were black, opaque, and angular were considered charcoal fragments (Patterson et al., 1987; Mooney and Tinner, 2011). Charcoal fragments were classified and counted according to two size categories based on the long axis of each fragment: 10–100 μm and $>100 \mu\text{m}$. Particles smaller than 75 μm^2 (or $\sim 10 \mu\text{m}$ long) were not counted due to the risk of false identification (Mooney and Tinner, 2011). Therefore, the charcoal signal primarily relates to the regional (10–100 μm) and local ($>100 \mu\text{m}$) fire signals and excludes extra-regional fires ($<10 \mu\text{m}$). Absolute charcoal abundances were calculated in the same manner as pollen concentrations (Stockmarr, 1971).

Defining plant–climate relationships

To objectively define the plant–climate relationships associated with the Pearly Beach pollen assemblage, we used the CREST (Climate REconstruction SofTware) method and software (Chevalier et al., 2014; Chevalier, 2019). For our analyses, we used botanical data obtained from the Global Biodiversity Information Facility (GBIF) database (<https://www.gbif.org>), specifically the curated data set of Chevalier (2020), and we used a regional subset of the Worldclim 2 climatology (Fick and Hijmans, 2017).

RESULTS

Stratigraphy and chronology

The particle size analysis results indicate that the 250 cm core predominantly comprises sands and silty sands with three distinct zones of pale coarser-textured sands at the top (0–25 cm), middle (130–160 cm), and base (235–250 cm) of the core (Figs. 3 and 4, Supplementary Appendix A). They are bounded by relatively homogeneous organic-rich silty sands. The exception being a thin lens of light-coloured coarser sand situated between 175 and 180 cm (Fig. 3).

The core spans the period ~ 25.3 cal ka BP to present (Fig. 3), encompassing much of the LGM (26.5–19 cal ka BP), Termination I (~ 19 –11.7 cal ka BP), and the Holocene (11.7–0 cal ka BP).

Pollen and microcharcoal

A total of 102 pollen taxa were identified from the 78 samples analysed. The pollen, non-pollen palynomorphs, microcharcoal, and particle size data (Figs. 4 and 5, Supplementary Appendix A) were divided based on CONISS analysis results and assemblage variability into four pollen assemblage zones (and three subzones). Pollen concentrations range between 2×10^3 and 33×10^3 grain/g, with peaks in concentration at 22.5–19 cal ka BP and 14–12 cal ka BP. No pollen was preserved from 11.6 to 8.5 cal ka BP.

The overall assemblage is characterised by variations in fynbos taxa (e.g., Proteaceae, Ericaceae, Restionaceae, *Cliffortia*, and *Stoebe*-type), coastal thicket elements (such as *Euclea*, *Morella*, and *Canthium*¹), succulent/drought-resistant elements (e.g., Aizoaceae, *Crassula*, and *Euphorbia*), and local wetland vegetation

(predominantly Cyperaceae, Juncaceae, and Haloragaceae), as well as more cosmopolitan pollen types such as Asteraceae and Poaceae. Ericaceae pollen is most prominent at the base of the sequence (pollen assemblage zone PB1-A; 25–21 cal ka BP), coinciding with the only significant presence of *Passerina*, relatively elevated proportions of *Stoebe*-type (which includes various *Stoebe* spp. and *Elytropappus* spp.) and low percentages of Proteaceae and Restionaceae. A further distinguishing feature of PB1-A is the generally greater proportions of coastal thicket taxa, particularly *Euclea* and Santalaceae, as well as discrete, relatively high peaks in *Dodonaea* and *Morella* from 22.5 to 21.5 cal ka BP. The isolated peaks in *Dodonaea* and *Morella* coincide with a large spike in *Crassula* (14%) and a smaller peak in Aizoaceae. Just before this phase, the highest counts and greatest concentrations of microcharcoal were recorded (from 23–22 cal ka BP). There is a small peak in Juncaceae percentages at the base of the sequence and peaks in Cyperaceae around 22 cal ka BP, although wetland taxa percentages are generally somewhat reduced for PB1-A.

For PB1-B (21–14.5 cal ka BP), we observe significantly elevated percentages of Restionaceae within the sand layer dating to ~ 20 –15.5 cal ka BP (Figs. 4 and 5), coinciding with generally reduced succulent/drought-resistant taxa and fynbos elements relative to PB1-A. The highest peak in the aquatic taxon Haloragaceae for the sequence (12%) and peaks in the coastal thicket taxa *Canthium* and *Morella* also characterise PB1-B. While *Dodonaea* reappears near the top of PB1-B, this taxon is recorded in more significant proportions within PB1-C (14.5–12 cal ka BP), together with relatively elevated percentages in coastal thicket indicators (e.g., *Canthium* and *Morella*) and the afrotemperate forest taxon *Clutia*. Fynbos (Ericaceae, Restionaceae, Proteaceae, and *Stoebe*-type) proportions remain relatively high for this period. The succulent/drought-resistant taxa *Crassula*, *Euphorbia*, and *Ruschia* all exhibit prominent peaks within this PB1-C.

Pollen was not found in sediments dating to the early Holocene (11.7–8 cal ka BP). For most of the mid- to late Holocene (PB1-D; ~ 7.7 –0 cal ka BP), other than Restionaceae, which remains relatively high, fynbos elements (particularly Ericaceae and *Passerina*) are represented in much lower proportions in comparison to the previous zones. The halophytic taxon Amaranthaceae peaks from 6 to 5 cal ka BP and is generally represented in high proportions within the whole of PB1-D. Coinciding with the peak in Amaranthaceae are peaks in *Ruschia*, *Crassula*, and microcharcoal concentrations. Microcharcoal concentrations and amounts (for both size classes) peak again from 2 to 1 cal ka BP. Asteraceae percentages are generally higher within PB1-D compared with the previous zones and reach a maximum for the sequence (38%) at ~ 4.2 cal ka BP. Wetland taxa generally exhibit no clear trends/changes other than a small peak in Blechnaceae at base of the zone at ~ 7.7 cal ka BP and peaks in Cyperaceae at ~ 5.8 and ~ 1.9 cal ka BP.

The most recent portion of the record, the last 500 years (PB1-D3), is substantially different from the rest of the Holocene section, being characterised by exceptionally high percentages of Proteaceae (up to 26%); distinct peaks in *Cliffortia*, Amaranthaceae, *Euclea*, *Morella*, and *Dodonaea*; and the appearance of *Sideroxylon* pollen.

DISCUSSION

The pollen results from the Pearly Beach sediment core reveal that distinct changes in vegetation composition occurred along the southwestern Cape coast since the onset of the LGM. The analysis

¹The *Canthium* pollen type includes *Canthium mundianum*, which has been renamed *Afrocanthium mundianum* (Lantz and Bremer, 2004).

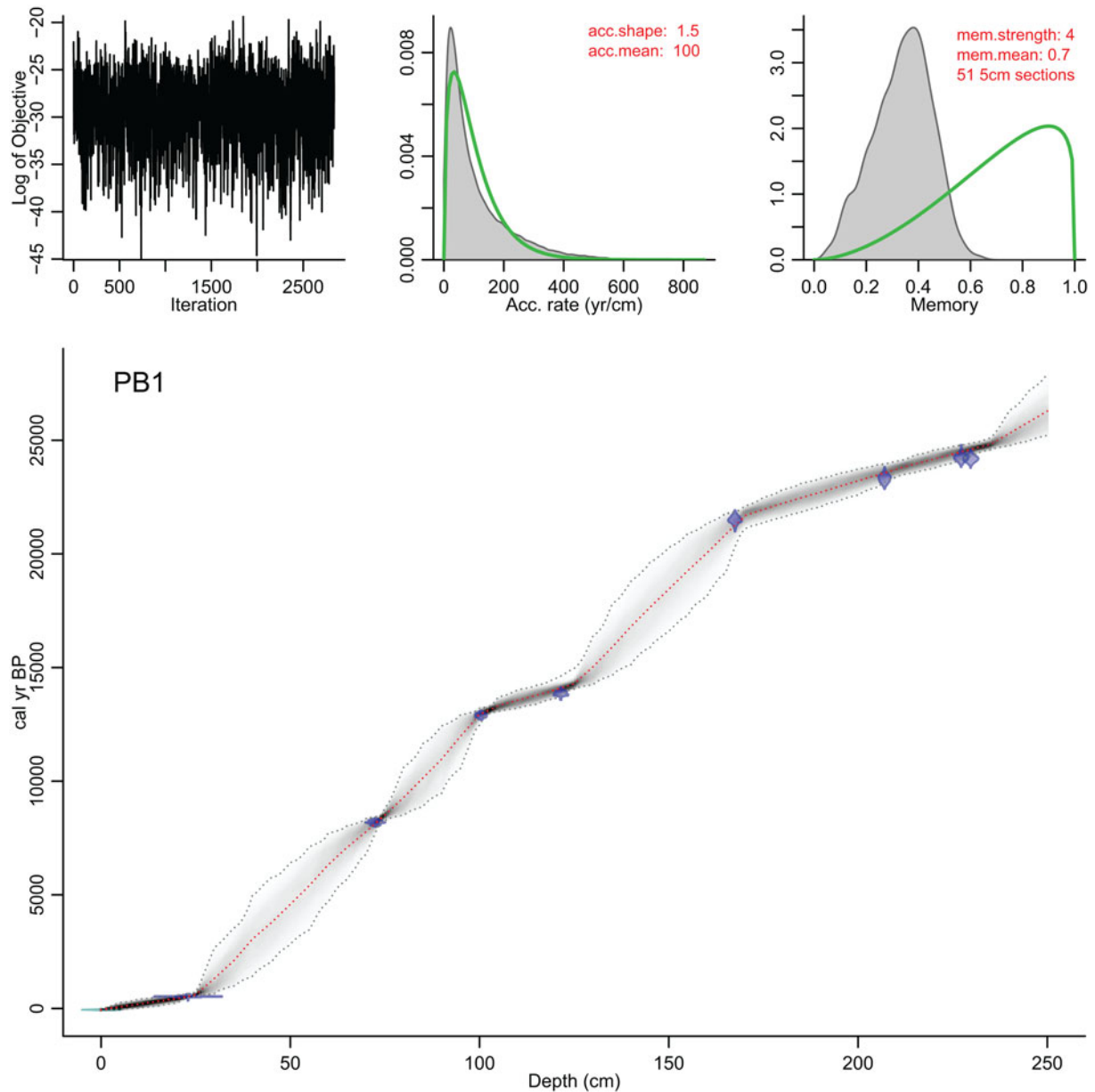


Figure 3. Age–depth model for Pearly Beach (PB1) using the rbacon (Blaauw and Christen, 2011). The blue areas represent the 2σ probability distributions of the calibrated ^{14}C ages, the greyscales indicate all likely age–depth models, grey dotted lines show the 95% confidence intervals, and the red dotted line shows the single “best” model based on the median age for each depth.

of contemporary climatic constraints on the identified taxa (Figs. 6 and 7) provides a framework for the interpretation of this record. Considerable variability in temperature and moisture availability may be inferred from these results, which are of particular importance in shedding new light on the LGM and Termination I in the region. The Holocene portion of the record is of significantly lower resolution, but it provides important context for understanding the climate and vegetation history of the site. As the site is located 2.5 km from the modern coastline and ~ 28.5 km from the LGM coastline (Spratt and Lisiecki, 2016; GEBCO Bathymetric Compilation Group, 2020), the potential impact of changing sea level should be considered when considering the Pearly Beach data. The gradient of the adjacent shelf is low and regular, and the coastline is predicted to have

encroached upon the site at a rate of ~ 1.6 km/ka since the LGM, achieving its current position at ~ 5 ka. Considering the position and palaeo-landscape of the site, factors such as increased continentality are unlikely to have been a significant factor, and a related progressive increase in moisture availability with reduced distance to the coast is not indicated by the pollen record, as will be described (Fig. 5). Similarly, rising sea levels would have raised base level and associated groundwater levels, but again the records do not indicate an increase in water availability with a rise in base level. Sea-level changes and the position of the site relative to the coast may also have had an impact on sedimentation regimes, with marine transgression resulting in an increase in marine and aeolian sands. Grain size results from the sediment core (Fig 4.), however, indicate no pattern that

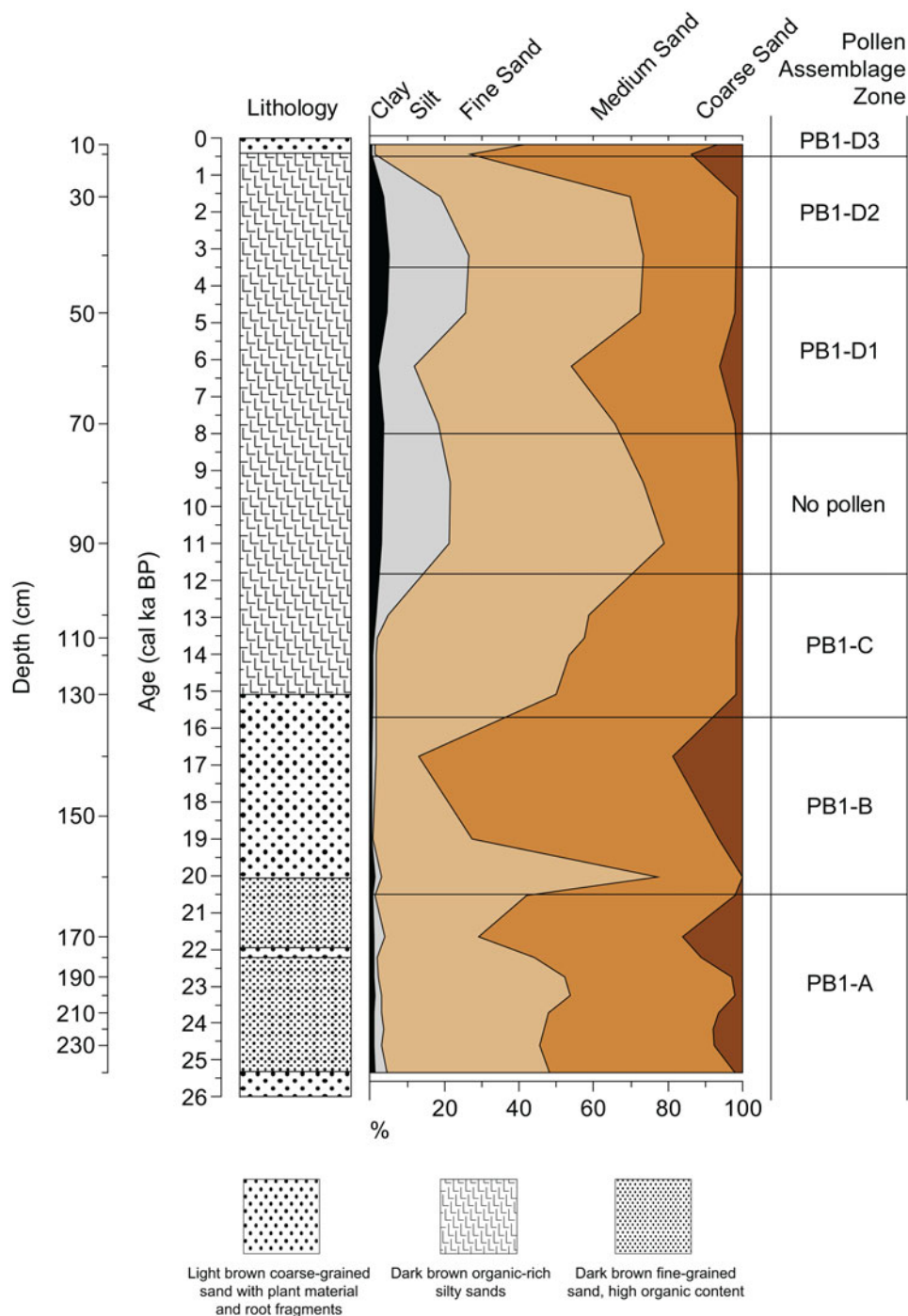


Figure 4. Pearly Beach 1 (PB1) particle size analysis data displayed as percentages of clay (0–2 μm), silt (2–20 μm), fine sand (20–200 μm), medium sand (200–500 μm), and coarse sand (500–2000 μm) plotted against interpolated age (cal ka BP) and composite depth (cm) with pollen assemblage zones indicated on the far right.

can be readily associated with sea-level change, such as an increase in the coarse sediment fraction. Thus, in the absence of specific evidence for a strong marine impact, the record is presently interpreted primarily in terms of climate.

The LGM (~25.3–19 cal ka BP)

Pollen from cold-tolerant fynbos taxa (e.g., *Stoebe*-type, *Passerina*, and *Ericaceae*) indicate that these plants were dominant features of the Pearly Beach landscape from 25.3 to 22.5 cal ka BP (Figs. 5–7).

This is consistent with other evidence of cooler conditions throughout southern Africa during the last glacial period and the LGM in particular (Heaton et al., 1986; Talma and Vogel, 1992; Stute and Talma, 1998; Truc et al., 2013; Chevalier and Chase, 2015). However, the presence of pollen from *Dodonaea*, a relatively frost-intolerant taxon (Valsecchi et al., 2013; Fig. 6), suggests that frost—if it occurred—was not common.

During this period, the coastal thicket group is dominated by a relatively high abundance of *Euclea* and *Santalaceae* pollen (likely *Thesium*, based on associations with increased fynbos

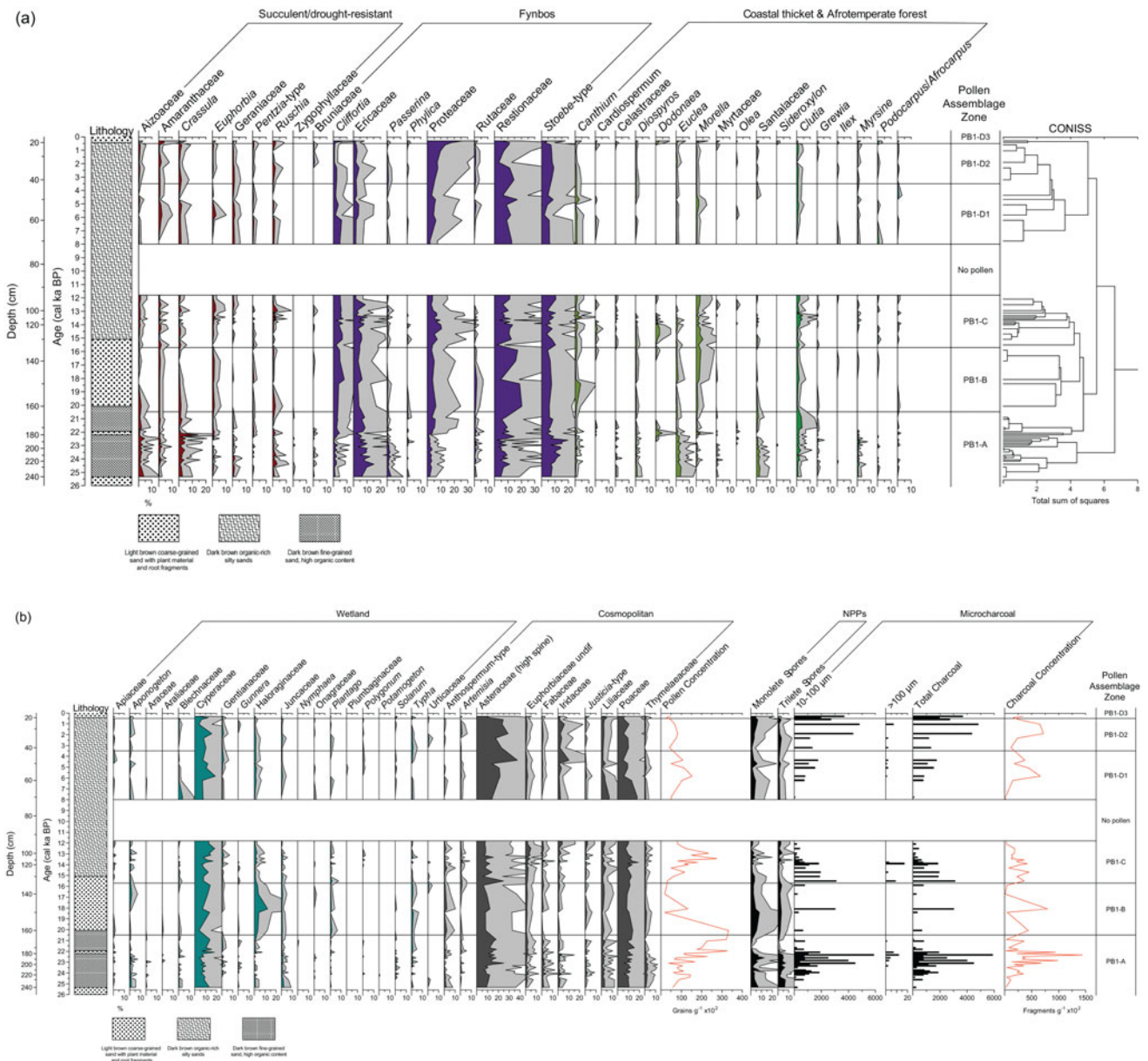


Figure 5. (a and b) Relative percentage pollen and microcharcoal diagrams for Pearly Beach (PB1). Taxa grouped according to general ecological affinities and are plotted against interpolated age (cal ka BP) and composite depth (cm). Taxa included in the Cosmopolitan ecological grouping that represent less than 2% for any given level were excluded, the full data set is presented in Supplementary Appendix A. Exaggeration curves are 3 \times , and zonation is based on the results of a constrained incremental sum of squares (CONISS) analysis.

representation at this time), which, coupled with the co-occurrence of *Ruschia* pollen, may reflect a relatively xeric coastal thicket composition (Boucher and Moll, 1981; Boucher, 1987; Cowling et al., 1999). While more mesic taxa such as *Morella*, *Canthium*, and the afrotemperate taxa *Podocarpus*/*Afrocarpus* and *Myrsine* are present, they are found only in relatively low proportions (Figs. 5–7). Cooler conditions at this time thus do not seem to be associated with either a significant decline in moisture availability (as has been inferred from charcoal data from Boomplaas Cave; Deacon et al., 1984; Scholtz, 1986). Nor, however, do they seem to reflect substantially wetter conditions during the LGM, as has been indicated by some palaeoclimate model simulations (Engelbrecht et al., 2019) and inferred from evidence elsewhere in the WRZ, such as Elands Bay Cave

(Cartwright and Parkington, 1997; Cowling et al., 1999; Parkington et al., 2000). Considered within the context of the record as a whole, *Euclaea* does exhibit a general positive relationship with microcharcoal concentrations (Fig. 5), suggesting that fire may also be a factor contributing to the dominance of *Euclaea* in the coastal thicket at this time. *Euclaea* (e.g., *E. racemosa*) may have been able to exert a competitive advantage over more mesic, less fire-adapted thicket taxa under a regime of more regular fire occurrence (Nzunda and Lawes, 2011).

The period from ~22.5 to 22 cal ka BP is characterised by high levels of succulent/drought-resistant pollen and decreased levels of both coastal thicket and afrotemperate forest taxa, indicating a period of relatively dry conditions (Figs. 5 and 8). High percentages of *Stoebe*-type pollen suggest this interval was also perhaps

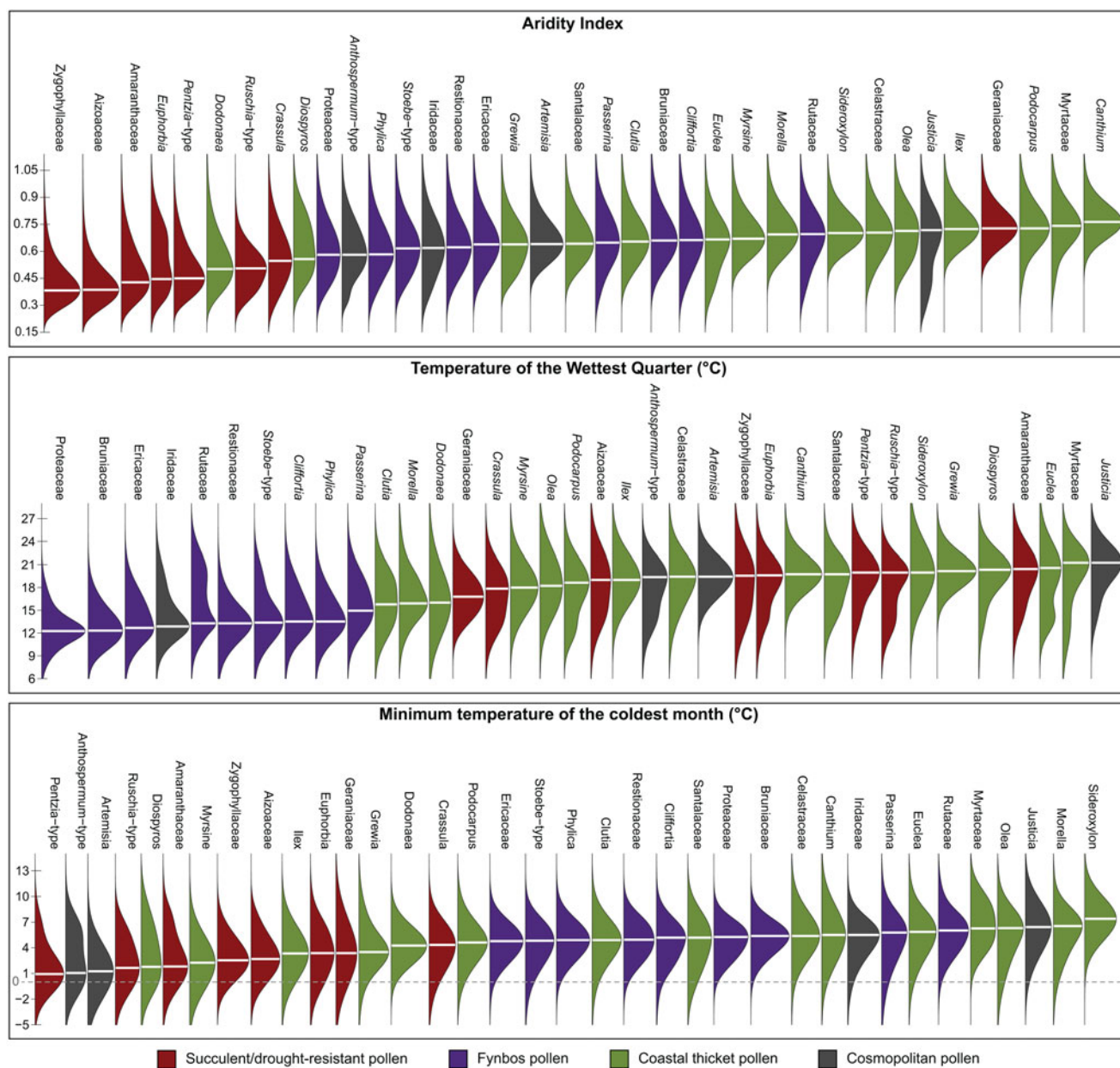


Figure 6. Probabilistic responses of the pollen taxa to three important regional climate determinants: the aridity index (Zomer et al., 2008; Trabucco and Zomer, 2019), the temperature of the wettest quarter (used as a proxy for the temperature of the growing season), and the minimum temperature of the coldest month (Fick and Hijmans, 2017). These responses were calculated following the probability density function (pdf) approach of Chevalier et al. (2014) and using data from the SANBI database (South African National Biodiversity Institute, 2020), restricted to the plant species that currently live in the study area (defined here as a box between 17° and 29°E and between 32° and 35°S).

the coolest of the last 25 kyr. At ~22 cal ka BP, this phase of cool and relatively dry conditions is disrupted abruptly by an episode of increased temperatures and humidity, as indicated by strong increases in *Morella* and *Dodonaea* pollen (Figs. 5 and 6). While brief, the timing of this event is consistent with episodes of increased humidity in other regional records at Seweweekspoort (Chase et al., 2017) and along the southwest African margin (Chase et al., 2019b).

The late LGM, from ~22 to 19 cal ka BP, is characterised by a further decline in coastal thicket and afrotemperate forest taxa and a dominance of Restionaceae pollen in association with greater contributions of medium- and coarse-grained sands (Figs. 4 and 5). These trends may reflect the ceding of the thicket

niche to Restionaceae species that are more tolerant of summer drought (e.g., *Thamnochortus*, which is common on dunes along the arid, winter rain-dominated west coast; Linder and Mann, 1998; South African National Biodiversity Institute, 2020). The thicket taxa *Morella* and *Canthium* begin to become more prominent at ~20 cal ka BP, suggesting the beginning of an increase in humidity that accelerates rapidly (reflected in substantial increases in these taxa) with the onset of Southern Hemisphere warming at ~19 ka.

In terms of drivers of the patterns of vegetation change observed in the Pearly Beach pollen record, the data are consistent with indications from elsewhere in southwestern Africa (e.g., Chase et al., 2015a, 2019b) that AMOC was a strong modulator

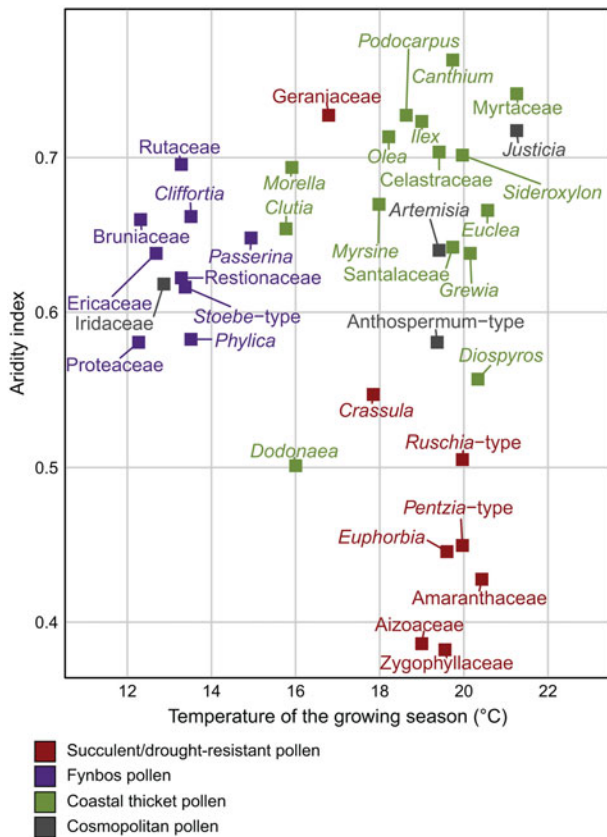


Figure 7. Biplot representing the climate optima (i.e., the climate value with the highest probability of presence) of the studied taxa for the temperature of the growing season (x-axis) (as represented by temperature of the wettest quarter) and aridity (y-axis; larger values associated with more humid conditions).

of global LGM conditions. At Pearly Beach, changes in the pollen record—while complex—are in accord with results from Namib Desert rock hyrax (*Procapra capensis*) middens, which indicate phases of relatively drier conditions (~24–22.5 cal ka BP and ~22–18 cal ka BP) demarcated by brief phases of increased humidity from ~24.5–24 cal ka BP and 22.5–22 cal ka BP before the beginning of Termination I (Chase et al., 2019b; Fig. 9).

At variance with the inference that the cool/cold boundary conditions of the terminal Pleistocene created relatively humid conditions in the southwestern Cape (van Zinderen Bakker, 1976; Cockcroft et al., 1987; Cowling et al., 1999), the Pearly Beach record suggests that phases of increased humidity correlate positively with increased temperature (Figs. 8 and 9). This likely relates to a combination of factors linked to a progressive buildup of heat in the South Atlantic and high southern latitudes associated with a weaker AMOC (Stocker and Johnsen, 2003; McManus et al., 2004; Ng et al., 2018). This warming—including the southeast Atlantic and oceans surrounding the southwestern Cape (Kim et al., 2003; Farmer et al., 2005; Dyez et al., 2014)—may have influenced regional climates through: (1) a southerly shift of the Atlantic Intertropical Convergence Zone (ITCZ) and African rainbelt (Broccoli et al., 2006), including a weakening of the southeasterly trade winds and a southerly shift of the Angola-Benguela Front (Kim et al., 2003; Fig. 1); (2) a poleward displacement of the Subtropical Front and westerlies storm track (Lee et al., 2011; Menviel et al., 2018) (likely also enabling increased Agulhas leakage into the SE Atlantic; Peeters et al., 2004; Caley et al., 2012), but a

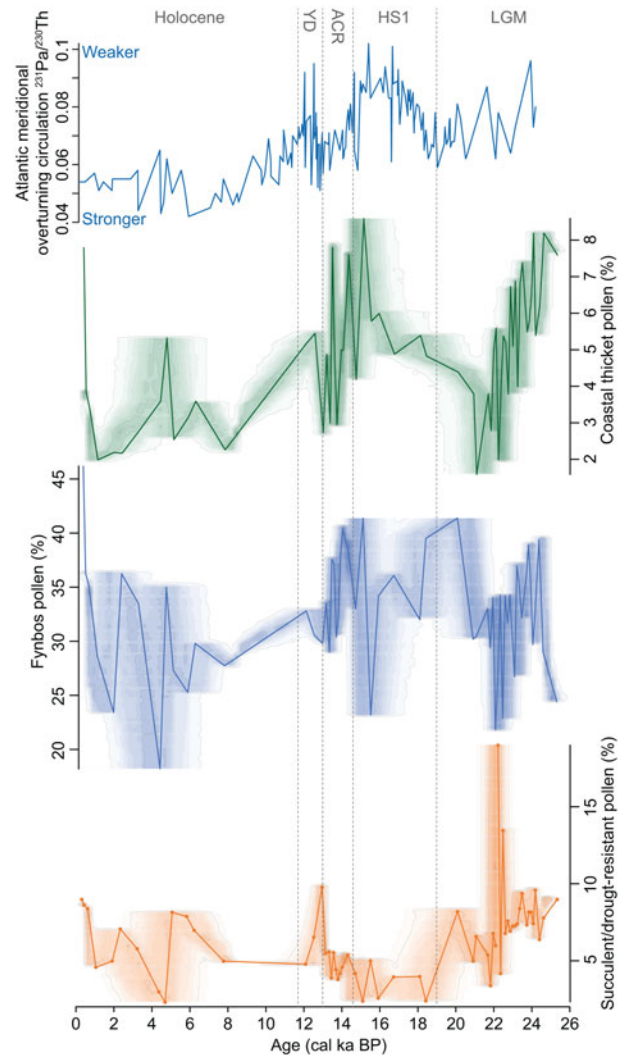


Figure 8. Primary pollen groups from Pearly Beach (PB1). Associated shading was obtained from proxy ghost analysis using rbacon software (v. 2.3.6; Blaauw and Christen, 2011) to express chronological uncertainties. The Holocene, Younger Dryas (YD), Antarctic Cold Reversal (ACR), and last glacial maximum (LGM) chronozones are indicated.

warming of the southwest Atlantic and waters upstream from the southwestern Cape, increasing moisture uptake by the frontal systems that bring winter rains to the Cape (Reason et al., 2002, 2006); and (3) increased evaporation and advection of moisture from southern coastal waters, fostering the development of localised precipitation systems (Jury et al., 1993, 1997). All these factors could result in a less-seasonal rainfall regime and a shorter/less intense drought season in the southwestern Cape (Chase et al., 2015b). At the subcontinental scale, it has been observed that warm events in the southeast Atlantic off Angola and Namibia are associated with increased rainfall along southern Africa's western margin and that these anomalies may extend inland significantly, particularly if easterly flow off the Indian Ocean is also high (Rouault et al., 2003). A critical dynamic may have thus been fostered between the warming and southward displacement of the Angola-Benguela Front (Fig. 1) and the increased moisture uptake of westerly frontal systems.

Today, cloud bands known as tropical-temperate troughs (TTTs) account for a significant proportion of southern Africa's summer rainfall and are a major mechanism for the poleward

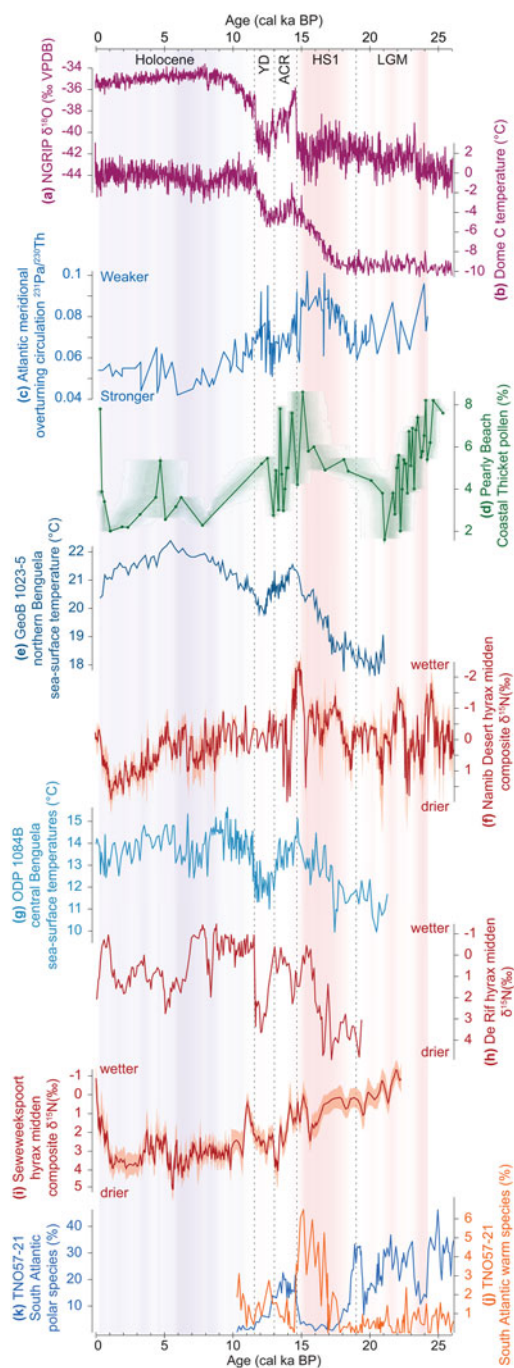


Figure 9. Comparison of records relevant to the context and climate dynamics associated with the changes observed in the Pearly Beach record. The last glacial maximum (LGM), Heinrich stadial 1 (HS1), Antarctic Cold Reversal (ACR), Younger Dryas (YD), and Holocene chronozones are indicated. Shading has been added to indicate the strength of Atlantic overturning circulation relative to the 25 ka mean (red = weaker, blue = stronger). Records shown are: (a) North Greenland Ice Core Project (NGRIP) oxygen isotope record (North Greenland Ice Core Project Members, 2004), (b) Antarctic temperature record from Dome C (Jouzel et al., 2007), (c) record of Atlantic overturning circulation strength (Ng et al., 2018), (d) the coastal thicket pollen record from Pearly Beach, shading from proxy ghost analysis using rbacon software (v. 2.3.6; Blaauw and Christen, 2011) to express chronological uncertainties, (e) sea-surface temperature record from the GeoB 1023-5 marine core (Kim et al., 2003), (f) Namib Desert rock hyrax midden nitrogen isotope record (Blaauw and Christen, 2011), (g) sea-surface temperature record from ODP 1084B marine core (Farmer et al., 2005), (h) De Rif rock hyrax midden nitrogen isotope record (Chase et al., 2011, 2015a), (i) Seweweekspoort rock hyrax midden nitrogen isotope record (Chase et al., 2017), (j and k) percentages of polar and warm water foraminiferal species in South Atlantic core TNO57-21 (Barker et al., 2009).

transfer of energy (Todd and Washington, 1999). The potential of TTTs and other forms of tropical temperate interactions (TTIs) to have been an important factor in determining synoptic-scale climate dynamics in southern Africa during the last glacial period has been highlighted and is considered to be a possible explanation for similarities in patterns of climate change across the continental interior (Chase, 2010; Chase et al., 2017). These types of synoptic systems have been identified as having an important influence on modern southern Cape climates (Engelbrecht et al., 2015), and similarities evident between the Pearly Beach record and records of climate change from sites in the Namib Desert (Chase et al., 2019b; Fig. 9) suggest that the interactions between tropical and temperate regions may have been enhanced during periods of elevated southeast Atlantic SSTs and that associated cloud bands and other related disturbances may have formed further to the southwest than is common today.

Termination I (~19–11.7 cal ka BP)

At Pearly Beach, the onset of Southern Hemisphere warming and the end of the LGM is associated with more abundant moisture, as indicated by the development of coastal thicket vegetation and a reduction in succulent/drought resistant pollen from ~19–13 cal ka BP (Figs. 5 and 8). In contrast to the thicket composition of the early LGM, *Canthium* is the dominant taxon at ~18.4 cal ka BP (Fig. 5). *Canthium* is most prevalent in humid coastal regions from the Knysna region eastward (South African National Biodiversity Institute, 2020), and at Pearly Beach it is a clear indicator of warmer, moister conditions (Fig. 7), likely implying significant contributions of summer rainfall as a result of the climate system dynamics, such as TTIs and as described above. Interestingly, *Canthium* quickly cedes dominance to *Morella*, which establishes itself as the most prominent thicket taxon for the period 18–14.5 cal ka BP, broadly coincident with the HS1 chronozone (~18.5–14.6 cal ka BP).

Morella and *Canthium* occupy very similar climatic niches, and the progression from *Canthium* to *Morella* dominance in the thicket taxa pollen spectrum may have been due to non-climatic mechanisms related to vegetation succession, as has been noted at other southern Cape sites (cf. Quick et al. 2016). *Morella* species likely do occur at the site (e.g., *M. quercifolia*) and are associated with stabilised sand dunes. *Canthium inerme* and *Afrocanthium mundianum* are associated with coastal forests and dune thicket but may have a closer association to active stream networks than *Morella*. The landscape surrounding Pearly Beach comprises a low-relief coastal platform (<30 m asl) occupied by alluvial and aeolian sediments—including an extensive semi-active to primarily dormant dune field—and a significant stream network associated with upland catchments to the north and northeast. The landscape dynamics of the immediate region therefore have potential to create a complex and changing mosaic of ecological niches. Therein, the observation that peaks in *Canthium* effectively bracket phases of *Morella* dominance may be associated with differences in the response time between fluvial systems and dune fields to changes in rainfall. While dune stabilisation under more humid conditions may be a protracted process, increased rainfall would have a much more immediate impact on fluvial activity and the development of riparian zones, thus potentially favouring the early establishment of *Canthium* over *Morella*. Once the dune fields became more stable, *Morella* would have become more prevalent. Conversely, increased aridity may have a more immediate impact on dune field vegetation, as fluvial networks may continue to be fed by rainfall

in the adjacent uplands and through groundwater discharge, maintaining higher levels of water availability at seeps and along channels.

Regardless of successional or landscape/hydrologic dynamics, the marked increase in *Canthium* and *Morella* pollen—and indeed coastal thicket taxa as a group—at ~18.5 cal ka BP, indicating a substantial increase in moisture availability, is coincident, and perhaps associated with a slowing AMOC (McManus et al., 2004; Ng et al., 2018) and a buildup of heat in the southern Atlantic (Fig. 9). As has been noted elsewhere (Chase et al., 2015a, 2019b), the response in terrestrial environments in southwestern Africa to changes in the AMOC associated with HS1 is not predicted to be immediate. The rapid slowdown in the AMOC at the beginning of HS1 resulted in a relatively slow, progressive buildup of heat in the South Atlantic and high southern latitudes, culminating in maximum temperatures being reached at the very end of HS1, at ~14.6 cal ka BP (Kim and Schneider, 2003; Farmer et al., 2005; Jouzel et al., 2007; Pedro et al., 2011; Fig. 9). As has been described for the LGM, these changes in SSTs in the Southeast Atlantic and oceans surrounding the southwestern Cape may have resulted in a less-seasonal rainfall regime. At such times, increased summer rainfall may have been derived from both localised precipitation systems (Jury et al., 1993, 1997) and the development of the aforementioned larger synoptic-scale TTTs /TTIs (Todd and Washington, 1999), which may have been more prevalent in the region, given elevated west coast SSTs (Fig. 9). At Pearly Beach, these changes are reflected in high coastal thicket taxa pollen percentages and a strong increase in *Dodonaea* pollen (Fig. 5), indicating warm, humid conditions under a less-seasonal rainfall regime.

Similarities with the deglacial record from Pearly Beach are observed across a wide range of terrestrial records not only from the southern and southwestern Cape (Chase et al., 2015a; Quick et al., 2016) and the western margin of southern Africa (Chase et al., 2015a, 2019b; Lim et al., 2016)—regions under the immediate influence of the South Atlantic Anticyclone and the westerlies—but also from the ARZ (Scholtz, 1986; Chase et al., 2017) and the SRZ (Chevalier and Chase, 2015), emphasising the subcontinental-scale influence of the slowdown of the AMOC during HS1 (Fig. 9).

HS1 ended at 14.6 ka, and at Pearly Beach this transition is marked by variable, declining levels of coastal thicket pollen and increases in pollen from xeric taxa such as *Ruschia* (Fig. 5). Coupled with increases in pollen from plants favouring cool/cold conditions—such as *Stoebe*-type and Ericaceae between ~13.9 and 12.6 cal kBP—the evidence seems to suggest that the increased AMOC strength (Ng et al., 2018) that triggered cooling in the southeast Atlantic (Kim and Schneider, 2003; Farmer et al., 2005) and the high southern latitudes (e.g., Jouzel et al., 2007)—the Antarctic Cold Reversal (Pedro et al., 2016)—resulted in relatively cool, dry conditions at Pearly Beach (Fig. 9). The subsequent Younger Dryas period is characterised by slight increases in pollen from both cool/cold and coastal thicket taxa, perhaps indicating a modest increase in winter rainfall. As has been noted elsewhere (Chase et al., 2015a), the magnitude of forcing associated with the Younger Dryas was substantially less than it was for HS1 and left an accordingly less distinct signature in most southwestern Africa records, with greater spatial heterogeneity.

The Holocene (7.8–0.3 cal ka BP)

No pollen was preserved in the sediments dating to ~12–7.8 cal ka BP in the Pearly Beach core. It could be speculated that the limited preservation of pollen within the Pearly Beach core during the

early Holocene was a response to increased aridity, as inferred from micromammalian data from Byneskranskop, an archaeological site 8 km northwest of Pearly Beach (Faith et al., 2018, 2020; Thackeray, 2020). Indications of relatively low moisture availability are also evident from further east within the Wilderness embayment (Martin, 1968; Quick et al., 2018), and the summer-rainfall zone (e.g., Holmgren et al., 2003), related, in part, to increased drought stress under warmer Holocene temperatures (Chevalier and Chase, 2016).

The resolution of the Holocene record allows for the identification of multimillennial trends, but it lacks the detail required to make definitive inferences regarding the primary mechanisms driving climate change. As a whole, coastal thicket pollen percentages are relatively low until the recent past, when a strong increase is observed at ~0.3 cal ka BP. This suggests generally drier Holocene conditions compared with the late Pleistocene, with a modest but notable increase in apparent humidity in the mid-Holocene, from ~6–4 cal ka BP (Figs. 5 and 9).

The recovery of high-resolution records from the southwestern Cape—from Katbakkies Pass (Chase et al., 2015b) and Pakhuis Pass (Chase et al., 2019a)—has enabled correlations with records for Southern Ocean SSTs and sea-ice extent (Nielsen et al., 2004) during the Holocene. These have been interpreted to indicate a phase of increased westerly influence during the mid-Holocene, which may account for the increased humidity at Pearly Beach. However, when considered in the context of other comparable records from the region, a pattern of marked spatial heterogeneity is observed (Chase et al., 2015a, 2019a), particularly between coastal and interior sites (Chase and Quick, 2018; Quick et al., 2018). Furthermore, the mid-Holocene in the Cape is a period of significant climatic variability, and while efforts have been made to establish diagnostic patterns of change that can be used to infer specific drivers (Chase et al., 2017, 2020; Chase and Quick, 2018), the Pearly Beach record currently lacks the requisite resolution to draw meaningful conclusions in this regard. It is evident that there are significant changes in the overall vegetation composition at Pearly Beach between the deglacial and Holocene, with a clear shift from ericaceous fynbos in the late Pleistocene to other structural types of fynbos (proteoid, restioid, and asteraceous) in the middle and late Holocene. These changes are likely in response to increased Holocene temperatures and relatively drier conditions compared with HS1 and at least some phases of the LGM.

The last 500 years are characterised by a significant increase in coastal thicket (e.g., *Euclea*, *Morella*, and *Sideroxylon*, as well as *Dodonaea*, comparable to the peaks during HS1) and represent the culmination of the steady rise in Proteaceae percentages across the Holocene (Fig. 5). While the abovementioned taxa suggest more humid conditions, consistent with coeval increases in temperature and humidity as indicated by the record as a whole, there is also an increase in Amaranthaceae and *Ruschia* pollen, suggesting at least some phases of more arid conditions and probably an increase in climate variability. The sharp increase in thicket taxa in the sample dated to ~0.3 cal ka BP is consistent with marked changes in inferred water availability in higher-resolution records from Bo Langvlei (du Plessis et al., 2020), Seweweekspoort (Chase et al., 2017), and the Namib region (Chase et al., 2019b). Again, however, the resolution of this portion of the Pearly Beach record—in terms of both pollen and radiocarbon samples—does not allow for a clearer attribution of this increase in thicket pollen to either an increase in summer rainfall following the Little Ice Age (LIA; 0.7–0.1 cal ka BP), as speculated at Bo Langvlei (du Plessis et al., 2020), or an increase in winter rainfall during the LIA, as inferred from diatom data at Verlorenvlei, on the west coast (Stager et al., 2012).

CONCLUSIONS

In this paper, we present new fossil pollen, microcharcoal, and sediment particle size data from a 25,000 year sediment core taken from a wetland at Pearly Beach, southwestern Cape coast of South Africa. The results reveal considerable variability in vegetation composition and, by inference, climate along the southwestern Cape coast since the onset of the LGM. We find that the Pearly Beach record is generally consistent with indications from elsewhere in southwestern Africa (Chase et al., 2015a, 2019b; Lim et al., 2016) that the AMOC, through its impact on regional oceanic and atmospheric circulation systems, was potentially a strong modulator of global LGM boundary conditions, resulting in phases of relatively drier conditions (~24–22.5 cal ka BP and ~22–18 cal ka BP) demarcated by brief phases of increased humidity (~24.5–24 cal ka BP and 22.5–22 cal ka BP). During Termination I, the marked increase in coastal thicket pollen at ~18.5 cal ka BP indicates a substantial increase in moisture availability, coincident and likely associated with a slowing AMOC and a buildup of heat in the southern Atlantic during HS1. The resolution of the Holocene portion of the record does not allow for definitive inferences regarding the primary mechanisms driving climate change, but it is evident that there are significant changes in the overall vegetation composition between the deglacial period and the Holocene, with a clear shift from ericaceous fynbos in the late Pleistocene to other structural types of fynbos (proteoid, restioid, and asteraceous) in the middle and late Holocene. These changes are likely in response to increased Holocene temperatures and relatively drier conditions.

Overall, the Pearly Beach record represents an important new contribution to a growing body of data that provides evidence for great spatial complexity in regional climatic responses and, more specifically, provides evidence that AMOC variability influence extended eastwards along the southwestern Cape coast at least as far as the modern boundary of the WRZ. It also provides a rare look at the response of lowland sectors of the mega-diverse CFR to major long-term climatic transitions.

Supplementary Material. The supplementary material for this article can be found at <https://doi.org/10.1017/qua.2021.31>.

Data Availability. The full pollen, charcoal, and particle size data sets are given in Supplementary Appendix A and will also be available on the Neotoma Palaeoecology data archive (<https://www.neotomadb.org>) as a contribution to the African Pollen Database.

Acknowledgments. We thank Carmen Kirchner for conducting the particle size analysis at the Department of Geography, Friedrich-Schiller-University, Jena. We also thank Rachid Cheddadi and Graciela Gil-Romera for assisting with recovery of the core.

Financial Support. LJQ acknowledges the financial assistance of the National Research Foundation (NRF) of South Africa, PAST (Palaeontological Scientific Trust), and the University of Cape Town. This study was funded in part by the European Research Council (ERC) under the European Union's Seventh Framework Programme (FP7/2007–2013)/ERC Starting Grant “HYRAX,” grant agreement no. 258657.

REFERENCES

- Barker, S., Diz, P., Vautravers, M.J., Pike, J., Knorr, G., Hall, I.R., Broecker, W.S., 2009. Interhemispheric Atlantic seesaw response during the last deglaciation. *Nature* 457, 1097–1102.
- Beal, L.M., De Ruijter, W.P., Biastoch, A., Zahn, R., 2011. On the role of the Agulhas system in ocean circulation and climate. *Nature* 472, 429–436.
- Bendle, J.M., Palmer, A.P., Thorndycraft, V.R., Matthews, I.P., 2019. Phased Patagonian Ice Sheet response to Southern Hemisphere atmospheric and oceanic warming between 18 and 17 ka. *Scientific Reports* 9, 4133–4133.
- Bergh, N.G., Cowling, R.M., 2014. Cenozoic assembly of the Greater Cape flora. In: Allsopp, N., Colville, J.F. and Verboom, G.A. (Eds.) *Fynbos: Ecology, Evolution, and Conservation of a Megadiverse Region*. Oxford University Press p. 93.
- Biastoch, A., Boning, C.W., Schwarzkopf, F.U., Lutjeharms, J.R.E., 2009. Increase in Agulhas leakage due to poleward shift of Southern Hemisphere westerlies. *Nature* 462, 495–498.
- Blaauw, M., Christen, J.A., 2011. Flexible paleoclimate age-depth models using an autoregressive gamma process. *Bayesian Analysis* 6, 457–474.
- Boucher, C., 1987. A Phytosociological Study of Transects through the Western Cape Coastal Foreland, South Africa. Unpublished PhD thesis, University of Stellenbosch, Stellenbosch, South Africa.
- Boucher, C., Moll, E.J., 1981. South African mediterranean shrublands. In: Di Castri, F., Goodall, D. W. and Specht, R. L. (Eds.) *Ecosystems of the World. Vol. 11, Mediterranean-type Shrublands*, Elsevier, Amsterdam pp. 233–248.
- Bradshaw, P.L., Cowling, R.M., 2014. Landscapes, rock types, and climate of the Greater Cape Floristic Region. In: Allsopp, N., Colville, J.F. and Verboom, G.A. (Eds.) *Fynbos: Ecology, Evolution and Conservation of a Megadiverse Region*, Oxford University Press pp. 26–46.
- Broccoli, A.J., Dahl, K.A., Stouffer, R.J., 2006. Response of the ITCZ to Northern Hemisphere cooling. *Geophysical Research Letters* 33. <https://doi.org/10.1029/2005GL024546>.
- Broecker, W.S., 1998. Paleocirculation during the last deglaciation: a bipolar seesaw? *Paleoceanography* 13, 119–121.
- Caley, T., Giraudeau, J., Malaizé, B., Rossignol, L., Pierre, C., 2012. Agulhas leakage as a key process in the modes of Quaternary climate changes. *Proceedings of the National Academy of Sciences USA* 109, 6835–6839.
- Carr, A.S., Boom, A., Chase, B.M., Meadows, M.E., Grimes, H.L., 2015. Holocene sea level and environmental change on the west coast of South Africa: evidence from plant biomarkers, stable isotopes and pollen. *Journal of Paleolimnology* 53, 415–432.
- Carr, A.S., Thomas, D.S.G., Bateman, M.D., 2006a. Climatic and sea level controls on late Quaternary eolian activity on the Agulhas Plain, South Africa. *Quaternary Research* 65, 252–263.
- Carr, A.S., Thomas, D.S.G., Bateman, M.D., Meadows, M.E., Chase, B., 2006b. Late Quaternary palaeoenvironments of the winter-rainfall zone of southern Africa: palynological and sedimentological evidence from the Agulhas Plain. *Palaeogeography, Palaeoclimatology, Palaeoecology* 239, 147–165.
- Cartwright, C., Parkington, J., 1997. The wood charcoal assemblages from Elands Bay Cave, Southwestern Cape: principles, procedures and preliminary interpretation. *South African Archaeological Bulletin* 52, 59–72.
- Chase, B., Boom, A., Carr, A., Chevalier, M., Quick, L., Verboom, A., Reimer, P., 2019a. Extreme hydroclimate gradients within the western Cape Floristic region of South Africa since the Last Glacial Maximum. *Quaternary Science Reviews* 219, 297–307.
- Chase, B.M., 2010. South African palaeoenvironments during marine oxygen isotope stage 4: a context for the Howiesons Poort and Still Bay industries. *Journal of Archaeological Science* 37, 1359–1366.
- Chase, B.M., Boom, A., Carr, A.S., Carré, M., Chevalier, M., Meadows, M.E., Pedro, J.B., Stager, J.C., Reimer, P.J., 2015a. Evolving southwest African response to abrupt deglacial North Atlantic climate change events. *Quaternary Science Reviews* 121, 132–136.
- Chase, B.M., Boom, A., Carr, A.S., Meadows, M.E., Reimer, P.J., 2013. Holocene climate change in southernmost South Africa: rock hyrax mid-dens record shifts in the southern westerlies. *Quaternary Science Reviews* 82, 199–205.
- Chase, B.M., Boom, A., Carr, A.S., Quick, L.J., Reimer, P.J., 2020. High-resolution record of Holocene climate change dynamics from southern Africa's temperate-tropical boundary, Baviaanskloof, South Africa. *Palaeogeography, Palaeoclimatology, Palaeoecology* 539, 109518.
- Chase, B.M., Chevalier, M., Boom, A., Carr, A.S., 2017. The dynamic relationship between temperate and tropical circulation systems across South Africa since the last glacial maximum. *Quaternary Science Reviews* 174, 54–62.

- Chase, B.M., Lim, S., Chevalier, M., Boom, A., Carr, A.S., Meadows, M.E., Reimer, P.J., 2015b. Influence of tropical easterlies in southern Africa's winter rainfall zone during the Holocene. *Quaternary Science Reviews* **107**, 138–148.
- Chase, B.M., Meadows, M.E., 2007. Late Quaternary dynamics of southern Africa's winter rainfall zone. *Earth-Science Reviews* **84**, 103–138.
- Chase, B.M., Meadows, M.E., Scott, L., Thomas, D.S.G., Marais, E., Sealy, J., Reimer, P.J., 2009. A record of rapid Holocene climate change preserved in hyrax middens from southwestern Africa. *Geology* **37**, 703–706.
- Chase, B.M., Quick, L.J., 2018. Influence of Agulhas forcing of Holocene climate change in South Africa's southern Cape. *Quaternary Research* **90**, 303–309.
- Chase, B.M., Quick, L.J., Meadows, M.E., Scott, L., Thomas, D.S.G., Reimer, P.J., 2011. Late-glacial interhemispheric climate dynamics revealed in South African hyrax middens. *Geology* **39**, 19–22.
- Chase, B., Niedermeyer, E.M., Boom, A., Carr, A.S., Chevalier, M., He, F., Meadows, M.E., Ogle, N., Reimer, P.J., 2019b. Orbital controls on Namib Desert hydroclimate over the past 50,000 years. *Geology* **47**, 867–871.
- Chevalier, M., 2019. Enabling possibilities to quantify past climate from fossil assemblages at a global scale. *Global and Planetary Change* **175**, 27–35.
- Chevalier, M., 2020. GBIF for CREST database https://figshare.com/articles/dataset/GBIF_for_CREAST_database/6743207/8, accessed 10 March 2020.
- Chevalier, M., Chase, B.M., 2015. Southeast African records reveal a coherent shift from high- to low-latitude forcing mechanisms along the east African margin across last glacial–interglacial transition. *Quaternary Science Reviews* **125**, 117–130.
- Chevalier, M., Chase, B.M., 2016. Determining the drivers of long-term aridity variability: a southern African case study. *Journal of Quaternary Science* **31**, 143–151.
- Chevalier, M., Cheddadi, R., Chase, B.M., 2014. CREST (Climate REconstruction SofTware): a probability density function (PDF)-based quantitative climate reconstruction method. *Climate of the Past* **10**, 2081–2098.
- Clark, P.U., Dyke, A.S., Shakun, J.D., Carlson, A.E., Clark, J., Wohlfarth, B., Mitrovica, J.X., Hostetler, S.W., McCabe, A.M., 2009. The last glacial maximum. *Science* **325**, 710–714.
- Climate System Analysis Group, 2021. Climate Information Platform. University of Cape Town, Cape Town <https://cip.csag.uct.ac.za/webclient2/app/>, accessed 7 March 2020.
- Cockcroft, M.J., Wilkinson, M.J., Tyson, P.D., 1987. The application of a present-day climatic model to the late Quaternary in southern Africa. *Climatic Change* **10**, 161–181.
- Cohen, A.L., Tyson, P.D., 1995. Sea surface temperature fluctuations during the Holocene off the south coast of Africa: implications for terrestrial climate and rainfall. *Holocene* **5**, 304–312.
- Cordova, C.E., Kirsten, K.L., Scott, L., Meadows, M., Lücke, A., 2019. Multi-proxy evidence of late-Holocene paleoenvironmental change at Princessvlei, South Africa: the effects of fire, herbivores, and humans. *Quaternary Science Reviews* **221**, 105896.
- Cowling, R., Campbell, B., Mustart, P., McDonald, D., Jarman, M., Moll, E., 1988. Vegetation classification in a floristically complex area: the Agulhas Plain. *South African Journal of Botany* **54**, 290–300.
- Cowling, R.M., 1992. *The Ecology of Fynbos: Nutrients, Fire, and Diversity*. Oxford University Press, Cape Town.
- Cowling, R.M., 1996. Flora and vegetation of Groot Hagelkraal (Bantamsklip site), Agulhas Plain. Unpublished report. Institute for Plant Conservation, University of Cape Town, Cape Town.
- Cowling, R.M., Cartwright, C.R., Parkington, J.E., Allsopp, J.C., 1999. Fossil wood charcoal assemblages from Elands Bay Cave, South Africa: implications for late Quaternary vegetation and climates in the winter-rainfall fynbos biome. *Journal of Biogeography* **26**, 367–378.
- Cowling, R.M., Lombard, A.T., 2002. Heterogeneity, speciation/extinction history and climate: explaining regional plant diversity patterns in the Cape Floristic Region. *Diversity and Distributions* **8**, 163–179.
- Cowling, R.M., Potts, A.J., Bradshaw, P.L., Colville, J., Arianoutsou, M., Ferrier, S., Forest, F., Fyllas, N.M., Hopper, S.D., Ojeda, F., 2015. Variation in plant diversity in mediterranean-climate ecosystems: the role of climatic and topographical stability. *Journal of Biogeography* **42**, 552–564.
- Cowling, R.M., Richardson, D.M., Schulze, R.E., Hoffman, M.T., Midgley, J.J., Hilton-Taylor, C., 1997. Species diversity at the regional scale. In: Cowling, R.M., Richardson, D.M., Pierce, S.M. (Eds.), *Vegetation of Southern Africa*. Cambridge University Press, Cambridge, pp. 447–273.
- Crowley, G.M., 1992. North Atlantic deep water cools the Southern Hemisphere. *Palaeoceanography* **7**, 489–497.
- Deacon, H.J., Deacon, J., Scholtz, A., Thackeray, J.F., Brink, J.S., 1984. Correlation of palaeoenvironmental data from the Late Pleistocene and Holocene deposits at Boomplaas Cave, southern Cape. In: Vogel, J.C. (Ed.), *Late Cainozoic Palaeoclimates of the Southern Hemisphere*. Balkema, Rotterdam, pp. 339–360.
- Deacon, H.J., Geleijnse, V.B., Thackeray, A.I., Thackeray, J.F., Tusenius, M.L., Vogel, J.C., 1986. Late Pleistocene cave deposits in the southern Cape: current research at Klasies River. In: Palaeoecology of Africa. Vol. 17. Proceedings of the 7th SASQUA Conference, Stellenbosch, 1985, pp. 31–37.
- du Plessis, N., Chase, B.M., Quick, L.J., Habertzettl, T., Kasper, T., Meadows, M.E., 2020. Vegetation and climate change during the Medieval Climate Anomaly and the Little Ice Age on the southern Cape coast of South Africa: Pollen evidence from Bo Langvlei. *The Holocene* **30**, 0959683620950444.
- Dyez, K.A., Zahn, R., Hall, I.R., 2014. Multicentennial Agulhas leakage variability and links to North Atlantic climate during the past 80,000 years. *Palaeoceanography* **29**, 1238–1248.
- Engelbrecht, C.J., Landman, W.A., Engelbrecht, F.A., Malherbe, J., 2015. A synoptic decomposition of rainfall over the Cape south coast of South Africa. *Climate Dynamics* **44**, 2589–2607.
- Engelbrecht, F.A., Marean, C.W., Cowling, R.M., Engelbrecht, C.J., Neumann, F.H., Scott, L., Nkoana, R., *et al.*, 2019. Downscaling Last Glacial Maximum climate over southern Africa. *Quaternary Science Reviews* **226**, 105879.
- Faegri, K., Iversen, J., 1989. *Textbook of Pollen Analysis*. 4th ed. Wiley, Chichester, UK.
- Faith, J.T., Chase, B.M., Avery, D.M., 2018. Late Quaternary micromammals and the precipitation history of the southern Cape, South Africa. *Quaternary Research* **91**, 848–860.
- Faith, J.T., Chase, B.M., Avery, D.M., 2020. Late Quaternary micromammals and the precipitation history of the southern Cape, South Africa: response to comments by F. Thackeray. *Quaternary Research* **95**, 154–156. *Quaternary Research* **95**, 157–159.
- Farmer, E.C., deMenocal, P.B., Marchitto, T.M., 2005. Holocene and deglacial ocean temperature variability in the Benguela upwelling region: implications for low-latitude atmospheric circulation. *Palaeoceanography* **20**. <https://doi.org/10.1029/2004PA001049>.
- Fick, S.E., Hijmans, R.J., 2017. WorldClim 2: new 1-km spatial resolution climate surfaces for global land areas. *International Journal of Climatology* **37**, 4302–4315.
- GEBCO Bathymetric Compilation Group 2020. The GEBCO_2020 Grid—a continuous terrain model of the global oceans and land. In: British Oceanographic Data Centre, N.O.C., NERC, UK (Ed.) doi:10/dtg3, accessed 7 March 2020.
- Goldblatt, P., 1978. An analysis of the flora of southern Africa: its characteristics, relationships, and origins. *Annals of the Missouri Botanical Garden* **65**, 369–436.
- Gordon, A.L., 1986. Inter-ocean exchange of thermocline water. *Journal of Geophysical Research: Oceans* **91**, 5037–5046.
- Gresse, P.G., Theron, J.N., 1992. The Geology of the Worcester Area: Explanations of Sheet 3319. 1:250 000. Geological Survey of South Africa, Pretoria.
- Grimm, E., 1987. CONISS: a Fortran 77 program for stratigraphically constrained cluster analysis by the method of incremental sum of squares. *Computers and Geosciences* **13**, 13–35.
- Grimm, E., 1991. Tilia and Tiliagraph. Version 1.7.16. Illinois State Museum Research and Collections Center, Springfield, IL.
- Heaton, T.H.E., Talma, A.S., Vogel, J.C., 1986. Dissolved gas paleotemperatures and 18O variations derived from groundwater near Uitenhage, South Africa. *Quaternary Research* **25**, 79–88.
- Henshilwood, C.S., Sealy, J.C., Yates, R., Cruz-Uribe, K., Goldberg, P., Grine, F.E., Klein, R.G., Poggenpoel, C., van Niekerk, K., Watts, I.,

2001. Blombos Cave, Southern Cape, South Africa: preliminary report on the 1992–1999 excavations of the Middle Stone Age levels. *Journal of Archaeological Science* **28**, 421–448.
- Hogg, A.G., Hua, Q., Blackwell, P.G., Niu, M., Buck, C.E., Guilderson, T.P., Heaton, T.J., Palmer, J.G., Reimer, P.J., Reimer, R.W., 2013. SHCal13 Southern Hemisphere Calibration, 0–50,000 cal yr BP. *Radiocarbon* **55**, 1889–1903.
- Holmgren, K., Lee-Thorp, J.A., Cooper, G.R.J., Lundblad, K., Partridge, T.C., Scott, L., Sthaldeen, R., Talma, A.S., Tyson, P.D., 2003. Persistent millennial-scale climatic variability over the past 25,000 years in Southern Africa. *Quaternary Science Reviews* **22**, 2311–2326.
- Irving, S.J.E., Meadows, M.E., 1997. Radiocarbon chronology and organic matter accumulation at Vankervelsvlei, near Knysna, South Africa. *South African Geographical Journal* **79**, 101–105.
- Jones, M.G.W., van Nieuwenhuizen, G.D.P., Day, J.A., 2002. Cape Action Plan for the Environment: Selecting Priority Wetlands for Conservation: The Agulhas Plain as a Case Study. *Freshwater Research Unit, Zoology Department, University of Cape Town, Cape Town*.
- Jouzel, J., Masson-Delmotte, V., Cattani, O., Dreyfus, G., Falourd, S., Hoffmann, G., Minster, B., et al., 2007. Orbital and millennial Antarctic climate variability over the past 800,000 years. *Science* **317**, 793–797.
- Jury, M., Rouault, M., Weeks, S., Schormann, M., 1997. Atmospheric boundary-layer fluxes and structure across a land-sea transition zone in south-eastern Africa. *Boundary-Layer Meteorology* **83**, 311–330.
- Jury, M.R., Valentine, H.R., Lutjeharms, J.R.E., 1993. Influence of the Agulhas Current on summer rainfall along the southeast coast of South Africa. *Journal of Applied Meteorology* **32**, 1282–1287.
- Kim, J.-H., Schneider, R.R., 2003. Low-latitude control of interhemispheric sea-surface temperature contrast in the tropical Atlantic over the past 21 kyr: the possible role of SE trade winds. *Climate Dynamics* **23**, 337–347.
- Kim, J.-H., Schneider, R.R., Mulitza, S., Müller, P.J., 2003. Reconstruction of SE trade-wind intensity based on sea-surface temperature gradients in the Southeast Atlantic over the last 25 kyr. *Geophysical Research Letters* **30**, 2144.
- Kirsten, K.L., Haberzettl, T., Wündsche, M., Frenzel, P., Meschner, S., Smit, A.J., Quick, L.J., Mäusbacher, R., Meadows, M.E., 2018. A multiproxy study of the ocean-atmospheric forcing and the impact of sea-level changes on the southern Cape coast, South Africa during the Holocene. *Palaeogeography, Palaeoclimatology, Palaeoecology* **496**, 282–291.
- Kirsten, K.L., Kasper, T., Cawthra, H.C., Strobel, P., Quick, L.J., Meadows, M.E., Haberzettl, T., 2020. Holocene variability in climate and oceanic conditions in the winter rainfall zone of South Africa—Inferred from a high resolution diatom record from Verlorenvlei. *Journal of Quaternary Science* **35**, 572–581.
- Kirsten, K.L., Meadows, M.E., 2016. Late-Holocene palaeolimnological and climate dynamics at Princessvlei, South Africa: evidence from diatoms. *The Holocene* **26**, 1371–1381.
- Klein, R.G., Cruz-Uribe, K., 2000. Middle and Later Stone Age large mammal and tortoise remains from Die Kelders Cave 1, Western Cape Province, South Africa. *Journal of Human Evolution* **38**, 169–195.
- Lantz, H., Bremer, B., 2004. Phylogeny inferred from morphology and DNA data: characterizing well-supported groups in Vanguerieae (Rubiaceae). *Botanical Journal of the Linnean Society* **146**, 257–283.
- Lee, S.Y., Chiang, J.C., Matsumoto, K., Tokos, K.S., 2011. Southern Ocean wind response to North Atlantic cooling and the rise in atmospheric CO₂: modeling perspective and paleoceanographic implications. *Paleoceanography* **26**. <https://doi.org/10.1029/2010PA002004>.
- Lim, S., Chase, B.M., Chevalier, M., Reimer, P.J., 2016. 50,000 years of vegetation and climate change in the southern Namib Desert, Pella, South Africa. *Palaeogeography, Palaeoclimatology, Palaeoecology* **451**, 197–209.
- Linder, H.P., 2005. Evolution of diversity: the Cape flora. *Trends in Plant Science* **10**, 536–541.
- Linder, H.P., Mann, D.M., 1998. The phylogeny and biogeography of *Thamnochortus* (Restionaceae). *Botanical Journal of the Linnean Society* **128**, 319–357.
- Linder, H.P., Meadows, M., Cowling, R.M., 1992. History of the Cape Flora. In: Cowling, R.M. (Ed.), *The Ecology of Fynbos: Nutrients, Fire and Diversity*. Oxford University Press, Cape Town, pp. 113–134.
- Lutjeharms, J., 1996. The exchange of water between the South Indian and the South Atlantic. In: Wefer, G., Berger, W.H., Siedler, G., Webb, D. (Eds.), *The South Atlantic: Present and Past Circulation*. Springer-Verlag, Berlin, pp. 125–162.
- Malan, J.A., 1990. *The stratigraphy and sedimentology of the Bredasdorp Group, Southern Cape Province*. Unpublished M.Sc. thesis, University of Cape Town.
- Marean, C.W., 2010. Pinnacle Point Cave 13B (Western Cape Province, South Africa) in context: the Cape Floral kingdom, shellfish, and modern human origins. *Journal of Human Evolution* **59**, 425–443.
- Martin, A.R.H., 1968. Pollen analysis of Groenvlei lake sediments, Knysna (South Africa). *Review of Palaeobotany and Palynology* **7**, 107–144.
- McManus, J.F., Francois, R., Gherardi, J.-M., Keigwin, L.D., Brown-Leger, S., 2004. Collapse and rapid resumption of Atlantic meridional circulation linked to deglacial climate changes. *Nature* **428**, 834–837.
- Meadows, M.E., Baxter, A.J., 2001. Holocene vegetation history and palaeoenvironments at Klaarfontein Springs, Western Cape, South Africa. *Holocene* **11**, 699–706.
- Meadows, M.E., Baxter, A.J., Parkington, J., 1996. Late Holocene environments at Verlorenvlei, Western Cape Province, South Africa. *Quaternary International* **33**, 81–95.
- Meadows, M.E., Seliane, M., Chase, B.M., 2010. Holocene palaeoenvironments of the Cederberg and Swartuggens mountains, Western Cape, South Africa: pollen and stable isotope evidence from hyrax dung middens. *Journal of Arid Environments* **74**, 786–793.
- Meadows, M.E., Sugden, J.M., 1991. A vegetation history of the last 14,000 years on the Cederberg, southwestern Cape Province. *South African Journal of Science* **87**, 34–43.
- Menviel, L., Spence, P., Yu, J., Chamberlain, M.A., Matear, R.J., Meissner, K.J., England, M.H., 2018. Southern Hemisphere westerlies as a driver of the early deglacial atmospheric CO₂ rise. *Nature Communications* **9**, 2503.
- Mix, A.C., Ruddiman, W.F., McIntyre, A., 1986. Late Quaternary paleoceanography of the tropical Atlantic, 2: the seasonal cycle of sea surface temperatures, 0–20,000 years B.P. *Paleoceanography and Paleoclimatology* **1**, 339–353.
- Mooney, S.D., Tinner, W., 2011. The analysis of charcoal in peat and organic sediments. *Mires and Peat* **7**, 1–18.
- Moore, P.D., Webb, J.A., Collinson, M.E., 1991. *Pollen Analysis*. 2nd ed. Blackwell Scientific, Oxford.
- Mucina, L., Adams, J.B., Knevel, I.C., Rutherford, M.C., Powrie, L.W., Bolton, J.J., van der Merwe, J.H., Anderson, R.J., Bornman, T.G., le Roux, A., 2006a. Coastal vegetation of South Africa. In: Mucina, L., Rutherford, M.C. (Eds.), *The Vegetation of South Africa, Lesotho and Swaziland*. South African National Biodiversity Institute, Pretoria, pp. 658–697.
- Mucina, L., Geldenhuys, C.J., 2006. Afrotemperate, subtropical and azonal forests. In: Mucina, L., Rutherford, M.C. (Eds.), *The Vegetation of South Africa, Lesotho and Swaziland*. South African National Biodiversity Institute, Pretoria, South Africa.
- Mucina, L., Rutherford, M.C., 2006. *The Vegetation of South Africa, Lesotho and Swaziland, Strelitzia*. South African National Biodiversity Institute, Pretoria.
- Mucina, L., Rutherford, M.C., Powrie, L.M., 2006b. Inland azonal vegetation. In: Mucina, L., Rutherford, M.C. (Eds.), *The Vegetation of South Africa, Lesotho and Swaziland*. South African National Biodiversity Institute, Pretoria, pp. 617–657.
- Mustart, P.J., Cowling, R.M., Albertyn, J., 2003. *Southern Overberg South African Wild Flower Guide* 8. Botanical Society of South Africa, Cape Town.
- Nakagawa, T., Brugiapaglia, E., Digerfeldt, G., Reille, M., De Beaulieu, J.-L., Yasuda, Y., 1998. Dense media separation as a more efficient pollen extraction method for use with organic sediment/deposit samples: comparison with the conventional method. *Boreas* **27**, 15–24.
- Neumann, F.H., Scott, L., Bamford, M.K., 2011. Climate change and human disturbance of fynbos vegetation during the late Holocene at Princess Vlei, Western Cape, South Africa. *The Holocene* **21**, 1137–1149.
- Ng, H.C., Robinson, L.F., McManus, J.F., Mohamed, K.J., Jacobel, A.W., Ivanovic, R.F., Gregoire, L.J., Chen, T., 2018. Coherent deglacial changes in western Atlantic Ocean circulation. *Nature Communications* **9**, 1–10.

- Nielsen, S.H., Koç, N., Crosta, X., 2004. Holocene climate in the Atlantic sector of the Southern Ocean: controlled by insolation or oceanic circulation? *Geology* **32**, 317–320.
- North Greenland Ice Core Project Members, 2004. High-resolution record of Northern Hemisphere climate extending into the last interglacial period. *Nature* **431**, 147–151.
- Nzunda, E., Lawes, M., 2011. Costs of resprouting are traded off against reproduction in subtropical coastal dune forest trees. *Plant Ecology* **212**, 1991–2001.
- Parkington, J., Cartwright, C., Cowling, R.M., Baxter, A., Meadows, M., 2000. Palaeovegetation at the Last Glacial Maximum in the Western Cape, South Africa: wood charcoal and pollen evidence from Elands Bay Cave. *South African Journal of Science* **96**, 543–546.
- Parkington, J.E., Poggenpoel, C., Buchanan, W.F., Robey, T., Manhire, A.H., Sealy, J., 1988. Holocene coastal settlement patterns in the Western Cape. In: Bailey, G., Parkington, J.E. (Eds.), *The Archaeology of Prehistoric Coastlines*. Cambridge University Press, Cambridge, pp. 22–41.
- Patterson, W.A., Edwards, K.J., Maguire, D.J., 1987. Microscopic charcoal as a fossil indicator of fire. *Quaternary Science Reviews* **6**, 3–23.
- Pedro, J.B., Bostock, H.C., Bitz, C.M., He, F., Vandergoes, M.J., Steig, E.J., Chase, B.M., Krause, C.E., Rasmussen, S.O., Markle, B.R., 2016. The spatial extent and dynamics of the Antarctic Cold Reversal. *Nature Geoscience* **9**, 51–55.
- Pedro, J.B., van Ommen, T.D., Rasmussen, S.O., Morgan, V.I., Chappellaz, J., Moy, A.D., Masson-Delmotte, V., Delmotte, M., 2011. The last deglaciation: timing the bipolar seesaw. *Climates of the Past* **7**, 671–683.
- Peeters, F.J.C., Acheson, R., Brummer, G.-J.A., de Ruijter, W.P.M., Schneider, R.R., Ganssen, G.M., Ufkes, E., Kroon, D., 2004. Vigorous exchange between the Indian and Atlantic oceans at the end of the past five glacial periods. *Nature* **430**, 661–665.
- Quick, L.J., Carr, A.S., Meadows, M.E., Boom, A., Bateman, M.D., Roberts, D.L., Reimer, P.J., Chase, B.M., 2015. A late Pleistocene–Holocene multiproxy record of palaeoenvironmental change from Still Bay, southern Cape Coast, South Africa. *Journal of Quaternary Science* **30**, 870–885.
- Quick, L.J., Chase, B.M., Meadows, M.E., Scott, L., Reimer, P.J., 2011. A 19.5 kyr vegetation history from the central Cederberg Mountains, South Africa: palynological evidence from rock hyrax middens. *Palaeogeography, Palaeoclimatology, Palaeoecology* **309**, 253–270.
- Quick, L.J., Chase, B.M., Wündsch, M., Kirsten, K.L., Chevalier, M., Mäusbacher, R., Meadows, M.E., Haberzettl, T., 2018. A high-resolution record of Holocene climate and vegetation dynamics from the southern Cape coast of South Africa: pollen and microcharcoal evidence from Eilandvlei. *Journal of Quaternary Science* **33**, 487–500.
- Quick, L.J., Meadows, M.E., Bateman, M.D., Kirsten, K.L., Mäusbacher, R., Haberzettl, T., Chase, B.M., 2016. Vegetation and climate dynamics during the last glacial period in the fynbos-afrotemperate forest ecotone, southern Cape, South Africa. *Quaternary International* **404**, 136–149.
- Rahmstorf, S., 2006. Thermohaline ocean circulation. In: Elias, S.A. (Ed.), *Encyclopedia of Quaternary Sciences* 5 Elsevier, Amsterdam.
- Reason, C.J.C., 2001. Evidence for the influence of the Agulhas Current on regional atmospheric circulation patterns. *Journal of Climate* **14**, 2769–2778.
- Reason, C.J.C., Landman, W., Tennant, W., 2006. Seasonal to decadal prediction of southern African climate and its links with variability of the Atlantic ocean. *Bulletin of the American Meteorological Society* **87**, 941–955.
- Reason, C.J.C., Rouault, M., Melice, J.L., Jagadheesha, D., 2002. Interannual winter rainfall variability in SW South Africa and large scale ocean-atmosphere interactions. *Meteorology and Atmospheric Physics* **80**, 19–29.
- Rebello, A.G., Boucher, C., Helme, N., Mucina, L., Rutherford, M.C., 2006. Fynbos biome. In: Mucina, L., Rutherford, M.C. (Eds.), *The Vegetation of South Africa, Lesotho and Swaziland*. South African National Biodiversity Institute, Pretoria, pp. 221–299.
- Rebello, A.G., Cowling, R.M., Campbell, B.M., Meadows, M.E., 1991. Plant communities of the Riversdale Plain. *South African Journal of Botany* **57**, 10–28.
- Rector, A.L., Reed, K.E., 2010. Middle and late Pleistocene faunas of Pinnacle Point and their paleoecological implications. *Journal of Human Evolution* **59**, 340–357.
- Reynolds, R.W., Smith, T.M., Liu, C., Chelton, D.B., Casey, K.S., Schlax, M.G., 2007. Daily high-resolution-blended analyses for sea surface temperature. *Journal of Climate* **20**, 5473–5496.
- Ritz, S.P., Stocker, T.F., Grimalt, J.O., Menviel, L., Timmermann, A., 2013. Estimated strength of the Atlantic overturning circulation during the last deglaciation. *Nature Geoscience* **6**, 208–212.
- Rouault, M., Florenchie, P., Fauchereau, N., Reason, C.J., 2003. South East tropical Atlantic warm events and southern African rainfall. *Geophysical Research Letters* **30**. <https://doi.org/10.1029/2002GL014840>.
- Rühls, S., Schwarzkopf, F., Speich, S., Biastoch, A., 2019. Cold vs. warm water route—sources for the upper limb of the Atlantic Meridional Overturning Circulation revisited in a high-resolution ocean model. *Ocean Science* **15**, 489–512.
- Schalke, H.J.W.G., 1973. The Upper Quaternary of the Cape Flats area. *Scripta Geologica* **15**, 1–57.
- Scholtz, A., 1986. *Palynological and Palaeobotanical Studies in the Southern Cape*. University of Stellenbosch, Stellenbosch, South Africa.
- Schweitzer, F.R., Wilson, M.L., 1982. Byneskranskop 1, a Late Quaternary Living Site in the southern Cape Province, South Africa. *Annals of the South African Museum* **88**, 1–203.
- Scott, L., 1982. Late Quaternary fossil pollen grains from the Transvaal, South Africa. *Review of Palaeobotany and Palynology* **36**, 241–278.
- Scott, L., Woodborne, S., 2007a. Pollen analysis and dating of Late Quaternary faecal deposits (hyraceum) in the Cederberg, Western Cape, South Africa. *Review of Palaeobotany and Palynology* **144**, 123–134.
- Scott, L., Woodborne, S., 2007b. Vegetation history inferred from pollen in Late Quaternary faecal deposits (hyraceum) in the Cape winter-rain region and its bearing on past climates in South Africa. *Quaternary Science Reviews* **26**, 941–953.
- South African National Biodiversity Institute, 2018. Vegetation Map of South Africa, Lesotho and Swaziland, <http://bgis.sanbi.org/SpatialDataset/Detail/1674>, date accessed: 7 March 2021.
- South African National Biodiversity Institute, 2020. Precip Plant Data. Version 1.0. Occurrence dataset <https://doi.org/10.15468/qfcyqk> accessed via GBIF.org on 10 May 2020.
- Spratt, R.M., Lisiecki, L.E., 2016. A Late Pleistocene sea level stack. *Climate of the Past* **12**, 1079–1092.
- Stager, J.C., Mayewski, P.A., White, J., Chase, B.M., Neumann, F.H., Meadows, M.E., King, C.D., Dixon, D.A., 2012. Precipitation variability in the winter rainfall zone of South Africa during the last 1400 yr linked to the austral westerlies. *Climate of the Past* **8**, 877–887.
- Stocker, T.F., 1998. The seesaw effect. *Science* **282**, 61–62.
- Stocker, T.F., Johnsen, S.J., 2003. A minimum thermodynamic model for the bipolar seesaw. *Paleoceanography* **18**. <https://doi.org/10.1029/2003PA000920>.
- Stockmarr, J., 1971. Tablets with spores used in absolute pollen analysis. *Pollen Spores* **13**, 615–621.
- Stuiver, M., Polach, H.A., 1977. Discussion: reporting of ^{14}C data. *Radiocarbon* **19**, 355–363.
- Stute, M., Talma, A.S., 1998. Glacial temperatures and moisture transport regimes reconstructed from noble gas and $\delta^{18}\text{O}$, Stampriet aquifer, Namibia. In: Isotope Techniques in the Study of Past and Current Environmental Changes in the Hydrosphere and the Atmosphere, IAEA Vienna Symposium 1997, Vienna, pp. 307–328.
- Taljaard, J., 1996. *Atmospheric Circulation Systems, Synoptic Climatology and Weather Phenomena of South Africa*. South African Weather Service Technical Paper 32. South African Weather Service, Pretoria, South Africa.
- Talma, A.S., Vogel, J.C., 1992. Late Quaternary paleotemperatures derived from a speleothem from Congo Caves, Cape Province, South Africa. *Quaternary Research* **37**, 203–213.
- Thackeray, J.F., 2020. Late Quaternary micromammals and the precipitation history of the southern Cape, South Africa—comment on the published paper by Faith et al., *Quaternary Research* (2019), Vol. 91, 848–860. *Quaternary Research* **95**, 154–156.
- Thwaites, R.N., Cowling, R.M., 1988. Soil-vegetation relationships on the Agulhas Plain, South Africa. *Catena* **15**, 333–345.
- Todd, M., Washington, R., 1999. Circulation anomalies associated with tropical-temperate troughs in southern Africa and the south west Indian Ocean. *Climate Dynamics* **15**, 937–951.
- Trabucco, A., Zomer, R.J., 2019. Global Aridity Index and Potential Evapotranspiration (ET0) Climate Database v. 2. https://figshare.com/articles/Global_Aridity_Index_and_Potential_Evapotranspiration_ET0_Climate_Database_v2/7504448/3, accessed 12 October 2019.

- Truc, L., Chevalier, M., Favier, C., Cheddadi, R., Meadows, M.E., Scott, L., Carr, A.S., Smith, G.F., Chase, B.M.**, 2013. Quantification of climate change for the last 20,000 years from Wonderkrater, South Africa: implications for the long-term dynamics of the Intertropical Convergence Zone. *Palaeogeography, Palaeoclimatology, Palaeoecology* **386**, 575–587.
- Tyson, P.D.**, 1986. *Climatic Change and Variability in Southern Africa*. Oxford University Press, Cape Town.
- Tyson, P.D., Preston-Whyte, R.A.**, 2000. *The Weather and Climate of Southern Africa*. Oxford University Press, Cape Town.
- Valsecchi, V., Chase, B.M., Slingsby, J.A., Carr, A.S., Quick, L.J., Meadows, M.E., Cheddadi, R., Reimer, P.J.**, 2013. A high resolution 15,600-year pollen and microcharcoal record from the Cederberg Mountains, South Africa. *Palaeogeography, Palaeoclimatology, Palaeoecology* **387**, 6–16.
- van Zinderen Bakker, E.M.**, 1953. *South African Pollen Grains and Spores*. Vol. 1. Balkema, Amsterdam–Cape Town.
- van Zinderen Bakker, E.M.**, 1956. *South African Pollen Grains and Spores*. Vol. 2. Balkema, Amsterdam–Cape Town.
- van Zinderen Bakker, E.M.**, 1976. The evolution of late Quaternary paleoclimates of Southern Africa. *Palaeoecology of Africa* **9**, 160–202.
- van Zinderen Bakker, E.M., Coetzee, J.A.**, 1959. *South African Pollen Grains and Spores*. Vol. 3. Balkema, Amsterdam–Cape Town.
- Walker, N.**, 1990. Links between South African summer rainfall and temperature variability of the Agulhas and Benguela Current systems. *Journal of Geophysical Research: Oceans* **95**, 3297–3319.
- Walker, N.D., Shillington, F.A.**, 1990. The effect of oceanographic variability on the South African weather and climate. *South African Journal of Science* **86**, 382–386.
- Willis, C.K., Cowling, R.M., Lombard, A.T.**, 1996. Patterns of endemism in the limestone flora of South African lowland fynbos. *Biodiversity and Conservation* **5**, 55–73.
- Wündsche, M., Haberzettl, T., Cawthra, H.C., Kirsten, K.L., Quick, L.J., Zabel, M., Frenzel, P., et al.**, 2018. Holocene environmental change along the southern Cape coast of South Africa – Insights from the Eilandvlei sediment record spanning the last 8.9kyr. *Global and Planetary Change* **163**, 51–66.
- Wündsche, M., Haberzettl, T., Kirsten, K.L., Kasper, T., Zabel, M., Dietze, E., Baade, J., et al.**, 2016. Sea level and climate change at the southern Cape coast, South Africa, during the past 4.2 kyr. *Palaeogeography, Palaeoclimatology, Palaeoecology* **446**, 295–307.
- Zomer, R.J., Trabucco, A., Bossio, D.A., van Straaten, O., Verchot, L.V.**, 2008. Climate change mitigation: a spatial analysis of global land suitability for clean development mechanism afforestation and reforestation. *Agriculture, Ecosystems and Environment* **126**, 67–80.